European Journal of Taxonomy 354: 1–30
https://doi.org/10.5852/ejt.2017.354
ISSN 2118-9773
www.europeanjournaloftaxonomy.eu
2017 · Kolicka M. *et al.*

Research article

urn:lsid:zoobank.org:pub:51C2BE54-B99B-4464-8FC1-28A5CC6B9586

A new species of freshwater Chaetonotidae (Gastrotricha, Chaetonotida) from Obodska Cave (Montenegro) based on morphological and molecular characters

Małgorzata KOLICKA[1,*], Piotr GADAWSKI[2] & Miroslawa DABERT[3]

[1]Department of Animal Taxonomy and Ecology, Institute of Environmental Biology, Adam Mickiewicz University Poznan, Umultowska 89, 61–614 Poznan, Poland.
[2]Department of Invertebrate Zoology and Hydrobiology, University of Łódź, Banacha 12/16, 90–237 Łódź, Poland.
[3]Molecular Biology Techniques Laboratory, Faculty of Biology, Adam Mickiewicz University Poznan, Umultowska 89, 61–614 Poznan, Poland.

[*]Corresponding author: kolicka@amu.edu.pl
[2]E-mail: gadawski@biol.uni.lodz.pl
[3]E-mail: mirkad@amu.edu.pl

[1]urn:lsid:zoobank.org:author:550BCAA1-FB2B-47CC-A657-0340113C2D83
[2]urn:lsid:zoobank.org:author:BCA3F37A-28BD-484C-A3B3-C2169D695A82
[3]urn:lsid:zoobank.org:author:8F04FE81-3BC7-44C5-AFAB-6236607130F9

Abstract. Gastrotricha is a cosmopolitan phylum of aquatic and semi-aquatic invertebrates that comprises about 820 described species. Current knowledge regarding freshwater gastrotrichs inhabiting caves is extremely poor and there are no extant data regarding Gastrotricha from Montenegro. We describe a new species from Obodska Cave, which is also the first record of a gastrotrich from this region. Due to its unusual habitat and morphological characteristics, this species may be important when considering the evolution and dispersion routes of Chaetonotidae Gosse, 1864 (*sensu* Leasi & Todaro 2008). We provide morphometric, molecular and phylogenetic data for the new species, together with photomicrographs and drawings.

Keywords. Balkan Peninsula, cave fauna, *Chaetonotus (Chaetonotus) antrumus* sp. nov., DNA barcode, Gastrotricha.

Kolicka M., Gadawski P. & Dabert M. 2017. A new species of freshwater Chaetonotidae (Gastrotricha, Chaetonotida) from Obodska Cave (Montenegro) based on morphological and molecular characters. *European Journal of Taxonomy* 354: 1–30. https://doi.org/10.5852/ejt.2017.354

Introduction

The eumetazoan meiofauna is considered a significant component of both rocky and soft bottoms of various natural aquatic ecosystems (Giere 2009). The meiofauna is an important source of food for macrofauna, small fish, juveniles of large fish and other epibenthic predators (Danovaro *et al.* 2007).

While trophic connections within meiofaunal assemblages are not particularly well studied, there is evidence to suggest that changes in community structure may affect higher and lower trophic levels (McCall & Fleeger 1995; Danovaro *et al.* 2007; Giere 2009). Moreover, meiofauna feeds on detritus, prokaryotes and microscopic eukaryotes and, therefore, plays essential roles in modulation of nutrient cycling processes, secondary production, sediment transport and detritus remineralization (Nozais *et al.* 2005; Danovaro *et al.* 2008). Due to their life cycle characteristics (small size, high turnover and lack of pelagic larval dispersal), these organisms are highly sensitive to environmental disturbance and respond rapidly to changes in food availability (Danovaro 1996; Fraschetti *et al.* 2006).

Within the meiofauna, gastrotrichs are microscopic free-living acoelomate eumetazoans with a total body length from 50 to 3500 µm (e.g., Kisielewski 1997; Balsamo *et al.* 2014; Kieneke & Schmidt-Rhaesa 2015). They inhabit all types of aquatic (fresh, brackish and marine waters) and semi-terrestrial ecosystems (e.g., peat bogs, sedge swamps and alder forests) throughout the world (Kisielewski 1981, 1997; Balsamo *et al.* 2008, 2014; Kieneke & Schmidt-Rhaesa 2015). Currently, there are about 820 known species of Gastrotricha belonging to two orders: Chaetonotida Remane, 1925 [Rao & Clausen, 1970] and Macrodasyida Remane, 1925 [Rao & Clausen, 1970] (Balsamo *et al.* 2009; Hummon & Todaro 2010; Kieneke & Schmidt-Rhaesa 2015; Todaro 2016). Gastrotrichs are known from across the globe, but not all regions have been studied equally. Europe is the most thoroughly studied continent with respect to the gastrotrich fauna, with ca 225 freshwater and ca 150 marine species described (Balsamo *et al.* 2015; Todaro 2016). However, some countries have been studied relatively well, while others are still blank areas on a map of gastrotrich research; for example, Poland is a country with one of the longest histories of detailed studies on gastrotrichs with 100 freshwater (Kisielewski 1997; Kolicka *et al.* 2013; Kolicka 2016) and 31 marine species currently known (Kisielewski 1997; Kolicka *et al.* 2014, 2015). At the same time there are no data available on the freshwater gastrotrich fauna of countries like Portugal, The Netherlands, Albania, Serbia and Montenegro (Balsamo *et al.* 2008, 2014, 2015). The number of species recorded on other continents, including the tropical regions, is even lower, especially when compared with the potential species richness of those areas: there are ca 75 freshwater species of Gastrotricha known from North America, ca 95 from South America, ca 65 from Asia and 10 species from Africa and Australia (Balsamo *et al.* 2008, 2014). Moreover, there are no data on the occurrence of Antarctic freshwater Gastrotricha (Balsamo *et al.* 2008, 2014; Todaro 2016).

Until now, there has been research on neither the freshwater nor the marine gastrotrich fauna in Montenegro or even in all of the Balkan Peninsula region (except Romania), despite the fact that both the high average annual temperature and the diversity of aquatic habitats in this area are favourable to the presence of diverse and abundant gastrotrich communities. During the past five decades, the biota inhabiting dark caves has attracted the attention of many biologists. Cave waters host a great variety of species associated only with this type of habitat, and are often characterized by very restricted geographic distributions (Jones *et al.* 2003). However, studies of the meiofauna of these peculiar biotopes are still very scarce. So far, Gastrotricha associated with inland caves has only been reported once (Vandel 1964), but not identified to the species level. The only comprehensive study on the gastrotrich fauna in a cave habitat was carried out in a sea cave, 'Grotta Piccola del Ciolo', by Todaro *et al.* (2006), who revealed that cave ecosystems can be hotspots of biodiversity and endemism for marine Gastrotricha. It is possible that further research of inland caves might result in similar conclusions regarding freshwater gastrotrichs. The new species described in this study will turn out to be crucial in considering representatives of Chaetonotida as typical cavernicolous organisms (Vandel 1964). Such recognition is highly important for further studies of the adaptation, evolution and dispersal routes of freshwater Gastrotricha.

Material and methods

Study area

This study was performed in the Obodska Cave (42°21.118′ N, 19°0.304′ E), which is located west of the Rijeka Crnojevica, in the cadastral municipality of Ljubotinj II, Montenegro (Fig. 1). The area is not cultivated and most of the natural vegetation is still intact. The landscape is mostly covered with deciduous forest. The climate is classified as humid subtropical (no dry season, hot summer), with a temperate warm and wet forest biozone (Bonada *et al.* 2008). The area is high in leptosol (lp), a weakly developed shallow soil. Cetinje field and its surroundings are inclined to the southeast toward Skadar Lake, which causes gravity flows of groundwater in that direction (Bonada *et al.* 2008). There are numerous caves and cavities in this region, indicating the degree and depth of karstification. Cavities are vertical or horizontal with an opening on the surface. In most cases they are located in areas of vertical cracks or fracture systems, where extended karst processes occur on the tectonic lines and on the contact zone between limestone and dolomite (Martinović 1964; Lješević 1968; Doderović *et al.* 2013).

Obodska Cave is a deep cave with the spring-fed Crnojevica River flowing through it (Figs 2–3). The major part of the cave is formed beneath Pecki Hill. The Crnojevica River flows into the cave through

Fig. 1. Map of Montenegro with the location of Obodska Cave.

a trench that plunges beneath the surface at the foot of Pecki Hill. Obodska Cave was created from stratified limestone, where edges of layers create horns visible on the vault. The sides and bottom of the upper channels are polished, in places, with narrow shelves on the horns of the layers. The cave is situated on three to five morphological levels (Palmer 1991). The total length of the cave is more than 350 meters and comprises three compartments connected by two siphons. The cave was formed through erosion by an underground river flowing along the initial chasm. The river flowed fast through stones and gravel in the whole cave and left holes in the solid rock (Martel 1893). Water in the cave leads to a humid microclimate (Obodska Cave has a precipitation/potential evapotranspiration index higher than 0.65) (Martel 1893; Lješević 1968; Mihavc 1983). Obod spring is characterized by a very variable flow that ranges from a minimum of 0.24 m^3/s to a maximum of 46 m^3/s. Typically, the minimum water level occurs in November or December, and the maximum occurs in March or April, or rarely in February. The first post-summer minimum peak in flow is caused by minimal autumn rainfall and high temperatures, while the maximum peak in flow is due to rain with snow and low temperatures. The low precipitation in Cetinje field and its adjacent surroundings results from a lack of water streams on land surface (Martinović 1964; Lješević 1969; Radulović & Radulović 2004).

The entrance to the cave is situated at 375 m above sea level, and the lowest point of the cave reaches an elevation of 244 m (192 m below the cave entrance). The main channel of the cave is divided by two siphons and creates the upper and lower channel. The lower channel is only partially passable (Mihavc 1983).

Obodska Cave was created in several morphological and hydrological stages. The main upper channel with a constant water flow was created during the first stage, when narrow pits were created at the bottom of the channel. The extension of the pits gradually allowed an increase of the amount of water that plunged through them and formed the second channel. This bifurcation of the channel has migrated during the second stage of development from a point close to the cave entrance to a point 45 meters from the entrance to the cave, where it is currently located. The third stage was characterized by the further scouring of the cave by the water flow, so that the upper part of the channel became dry. It is impossible to observe the bifurcation, because the lower water plunges through sinkholes in the bottom

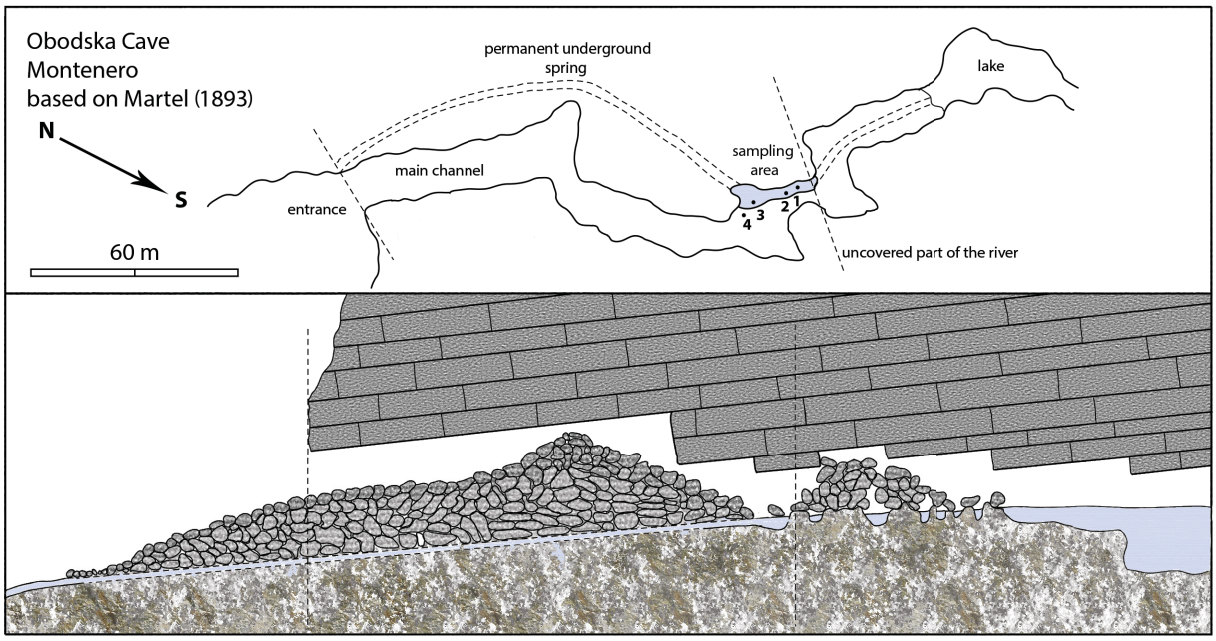

Fig. 2. Scheme of Obodska Cave. 1, 2, 3, 4 = sampling localities.

and flows through cave channels underground. All this shows that there is another, lower cave channel, which today contains warm water. The genesis of this cave and its water flow reflect the typical lowering of the underground water flow in karst. Finally, it should be noted that the regime of the Crnojevic springs, which emerge from the cave, is very uneven. The flow of water fluctuates from 0.03 to 2 m^3 per year (Dinić 1965). A few endemic species of invertebrates are known from this cave, e.g., Amphipoda: *Metohija carinata* Absolon, 1927; Gastropoda: *Plagigeyeria montenigrina* Bole, 1961 and Coleoptera: *Adriaphaenops stirni* Pretner, 1959. They occur only there or in a few other caves on the Adriatic coast (Pretner 1972; Pešić 2010; Hou & Sket 2015).

Sampling and documentation

One sample of approximately 50–70 cm^3 from the top layer of the bottom sediment, together with approximately 100–120 cm^3 of ambient water, was collected from each of 4 sites within one locality on 29 July 2015. Each sample was placed in a 200 cm^3 plastic container. The sampling area was situated at the end of the middle compartment approximately 150 meters from the entrance to the cave. Samples were collected in an area not covered by stones and gravel close to the second siphon, connecting the second and third compartments. Four samples were collected from different parts of the river channel: (1) in the main channel at a depth of 0.4 m, (2) from the main channel at a depth of 0.25 m, (3) from shallows at a depth of 0.1 m, and (4) from pockets among stones and gravel. The last sample (4) was collected from a place where water filled the space between stones and boulders which had fallen from the roof of the cave. The sampling locations were separated by no less than 2 m (Fig. 2).

Water parameters, such as temperature, pH, electrolytic conductivity and dissolved oxygen content, were measured in the field with an Elmetron CX-401 multiparametric sampling probe; BOD5 by Winkler's method, and NH_4, NO_3, PO_3 with a Slandi LF205 photometer. The collected samples were subsequently placed in an insulated box and transported to the laboratory, where the samples were oxygenated and held at 12°C in order to create conditions similar to those at the sampling site. Within 10 days after collection, a total of 2 cm^3 of sediment from each sample was searched for gastrotrichs. Specimens were extracted with a micropipette under an Olympus SZ51 stereo microscope. All specimens were observed, photographed and documented alive with an Olympus BX53 microscope equipped with phase contrast and an Array Artcam 500 digital camera or a Leica DM 5500 B microscope equipped with

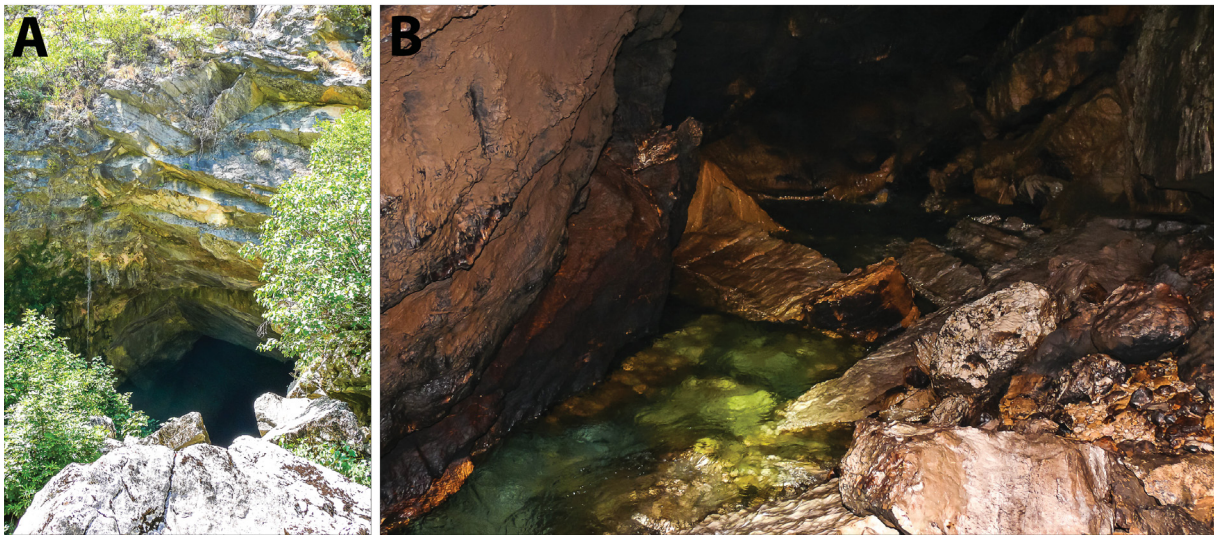

Fig. 3. Photographs of Obodska Cave. **A**. Entrance to the Cave. **B**. Sampling area inside the Cave. (Photographs by Przemysław Śmietana.)

differential interference contrast (DIC) and a Leica DFC 450 digital camera. Morphometric characters were measured in cellSens Entry 1.11 software (Olympus). All measurements are given in micrometers (µm) and all formulas used are given as a percentage (%).

Granulometric analyses

To determine the grain-size properties, the granulometric protocol described by Buchanan (1984) was applied. The grain-size statistics were calculated through Gradistat software using a logarithmic method of moments (Blott & Pye 2001) and sediments were classified according to the Folk and Ward system (Folk & Ward 1957). The organic matter content of the same sediment samples was determined using the combustion method. The main results of the granulometric analyses are provided in Table 1.

Morphological analyses

A morphological feature was measured only if its orientation was conducive to accurate measurement. Ranges of measurements are presented. Each of the specimens was documented by means of a set of photomicrographs. The species description follows the convention of Hummon *et al.* (1992), in which the longitudinal distance of a morphological character from the anterior end is expressed as percentage units (U) of the animal's total length (i.e., the distance of the character from the anterior end, divided by the total body length, and multiplied by 100). The identification of gastrotrichs, their morphological study and terms follows Kisielewski (1981, 1991, 1997) and Kolicka *et al.* (2016). The terms describing the shape of furcal branches and furcal indentation follows Roszczak (1969). In this paper, the following formula describing the distribution of scales was used:

$$\text{Ratio of scales distribution} = \frac{\text{total number of longitudinal alternating rows of scales}}{\text{number of scales in central longitudinal row}} \times 100\%$$

as well as the pharynx formulae according to Kisielewski (1991):

$$a = \frac{\text{width of anterior thickening}}{\text{pharynx length}} \times 100\% \qquad n = \frac{\text{width of pharynx narrowing}}{\text{pharynx length}} \times 100\%$$

$$m = \frac{\text{width of middle pharynx}}{\text{pharynx length}} \times 100\% \qquad p = \frac{\text{width of anterior thickening}}{\text{pharynx length}} \times 100\%$$

Abbreviations used: D = dorsal; DL = dorsolateral; L = lateral; LV = ventrolateral; V= ventral.

The new species proposed in this paper is described by the first author only. This solution is consistent with chapter 11, article 50 of the International Code of Zoological Nomenclature (The International Commission on Zoological Nomenclature 1999).

Molecular analyses

Total genomic DNA was extracted from three single specimens of the new species using the DNeasy Blood and Tissue Kit (Qiagen GmbH, Hilden, Germany) as described by Dabert *et al.* (2008). A 628 bp fragment of the mitochondrial cytochrome *c* oxidase subunit I (COI) gene was amplified with a 1:1 mixture of two forward primers, bcdF08 and bcdF09 (Kolicka *et al.* 2016), and reverse primer bcdR04 (Dabert *et al.* 2010). A fragment coding for both internal transcribed spacers (ITS1-5.8S rDNA-ITS2) was amplified with ITS1_18S and ITS2_28S primers (Navajas *et al.* 1998). A complete sequence of 18S rRNA was amplified in two overlapping fragments using 18Sfw/rev960 and fw390/rev18S primer pairs (Dabert *et al.* 2010), respectively. A 2381 bp fragment of 28S rRNA was amplified using the primer pair 28SF0001/28SR2850 (Dabert *et al.* 2016). For primer details see Table 2. PCRs were carried out in 10 µl reaction volumes containing 5 µl of the Type-it Microsatellite PCR Kit (Qiagen), 0.5 µM of each primer and 4 µl of the DNA template using a thermocycling profile with one cycle

Table 1. Main results of sediment sample granulometric analyses. All measurements are given in micrometres (μm); indicators are given as a percentage (%) and italicized.

Sites		**1**	**2**	**3**	**4**
Mean		Coarse sand	Very coarse sand	Medium sand	Very coarse sand
	(M_G)	859.5	1235.8	384.2	1318.4
Sorting		Moderately sorted	Well sorted	Poorly sorted	Very well sorted
	(σ_G)	1.748	1.277	2.190	1.071
Skewness		Symmetrical	Very fine skewed	Fine skewed	Very coarsely skewed
		-0.016	-2.521	-0.104	1.076
Kurtosis		Mesokurtic	Very fine skewed	Leptokurtic	Very platykurtic
		1.080	1.069	1.131	-0.596
Organic matter		*6.61*	*2.64*	*4.09*	*2.63*

of 5 min at 95°C followed by 40 steps of 30 s at 95°C, 90 s at 50°C, 1 min at 72°C, and with a final step of 5 min at 72°C for all reactions. After amplification, the PCR products were diluted with 10 μl of MQ water; 5 μl of the diluted PCR reaction was analysed by electrophoresis on 1% agarose gel. Samples containing visible bands were purified with exonuclease I and Fast alkaline phosphatase (Fermentas) and sequenced using the BigDye Terminator v3.1 kit and the ABI Prism 3130xl Genetic Analyzer (Applied Biosystems), following the manufacturer's instructions. Individual sequence reads were aligned and manually assembled into contigs in ChromasPro v. 1.32 (Technelysium) and GeneDoc v. 2.7.000 (Nicholas & Nicholas 1997). Genetic distance among the COI sequences was estimated using the Kimura 2-parameter model as implemented in MEGA 7 (Kimura 1980; Tamura *et al.* 2013).

Phylogenetic analyses

The nucleotide blast search of COI, 18S and 28S rRNA sequences of *Chaetonotus (Chaetonotus) antrumus* sp. nov. suggested *Chaetonotus* sp. 1 (in Kånneby, Todaro & Jondelius 2013), *Chaetonotus (Chaetonotus)* cf. *sphagnophilus* Kisielewski, 1981 and *Chaetonotus (Chaetonotus)* cf. *laroides* Marcolango, 1910 as the most similar taxa. Therefore, in our phylogenetic analyses we used representatives of the main clades reconstructed in the published molecular phylogeny of Chaetonotidae (Kånneby *et al.* 2013; Kolicka *et al.* 2016). As the outgroup we used sequences of *Aspidiophorus polystictos* Balsamo & Todaro, 1987, which has been reconstructed as the sister group to all other species of Chaetonotidae by Kånneby *et al.* (2013). In total, our data set consisted of 4881 nucleotide positions for 55 terminals (Table 3) and involved COI+18S+28S markers. ITS sequences were excluded from the data set because of the lack of sequence data for this marker for most species included in the phylogenetic analysis.

Choice of an appropriate model of DNA sequence evolution for 18S and 28S rDNA was made using jModeltest 0.11 (Posada 2008); the GTR + I + G model was appropriate for both markers. For COI DNA sequences the two-rate codon-based model was applied (Goldman & Yang 1994) with invertebrate mtDNA genetic code. Tree inference was performed using Bayesian Inference with Markov Chain Monte Carlo (BI), with the appropriate substitution model for each partition. Four independent chains were run on a parallel version of MrBayes 3.2 (Ronquist *et al.* 2012). Each run of the BI analyses was performed in 3–10 × 10^6 generations, and the trees were sampled every 1000th generation. The final 50% majority rule consensus tree was generated after discarding the 25% burn-in fraction of initial trees after assessing the chain convergence in Tracer v.1. (Rambaut & Drummond 2007) judged by the average standard deviation of split frequencies dropping below 0.01. Tree editing was performed using FigTree 1.4.2 (Rambaut 2014).

Table 2. PCR primers used in this study; A and S refer to amplifying and sequencing, respectively.

Primer name	Sequence (5'–3')	Product	Use	Source
bcdF08	CGATGRTTTTTTTCHACWAACCAYAARGATATCGG	COI	A	Kolicka *et al.* 2016
bcdF09	CGATGRTTTTTTTCHACWAACCAYAARGACATTGG	COI	A, S	Kolicka *et al.* 2016
bcdR04	TATAAACYTCDGGATGNCCAAAAAA	COI	A, S	Dabert *et al.* 2008
ITS1_18S	AGAGGAAGTAAAAGTCGTAACAAG	ITS	A, S	Navajas *et al.* 1998
ITS2_28S	ATATGCTTAAATTCAGGGGG	ITS	A, S	Navajas *et al.* 1998
18Sfw	CTTGTCTCAAAGATTAAGCCATGCA	18S rDNA	A, S	Dabert *et al.* 2010
rev480	GTTATTTTTCGTCACTACCT	18S rDNA	S	Dabert *et al.* 2010
fw390	AATCAGGGTTCGATTCCGGAGA	18S rDNA	A, S	Dabert *et al.* 2010
rev960	GACGGTCCAAGAATTTCAC	18S rDNA	A, S	Dabert *et al.* 2010
for1300	TGCATGGCCGTTCTTAGTTG	18S rDNA	S	Dabert *et al.* 2010
rev1460	CATCACAGACCTGTTATTGC	18S rDNA	S	Dabert *et al.* 2010
rev18S	TGATCCTTCCGCAGGTTCACCT	18S rDNA	A, S	Dabert *et al.* 2010
28SF0001	ACCCVCYNAATTTAAGCATAT	28S rDNA	A	Dabert *et al.* 2016
1634LReverse	ATTCGGCAGGTGAGTTGTTACA	28S rDNA	S	Telford *et al.* 2003
1200F	CCCGAAAGATGGTGAACTATGC	28S rDNA	S	Telford *et al.* 2003
2450R	GCTTTGTTTTAATTAGACAGTCGGA	28S rDNA	A, S	Telford *et al.* 2003
28SR2850	GTGGTTTCGCTAGATAGTAGATA	28S rDNA	A, S	Dabert *et al.* 2016
300F	CAAGTACCGTGAGGGAAAGTTG	28S rDNA	S	Telford *et al.* 2003
300R	CAACTTTCCCTCACGGTACTTG	28S rDNA	S	Telford *et al.* 2003
1200R	GCATAGTTCACCATCTTTCGG	28S rDNA	S	Telford *et al.* 2003
UJR2176	CGGATCTAATTTGCCGACTTCCCTTA	28S rDNA	S	Telford *et al.* 2003
1600F	AGCAGGACGGTGGCCATGGAAG	28S rDNA	S	Telford *et al.* 2003

Results

Gastrotrichs, belonging to only one species, were present in two of the four sampled sites: Site 1 (9 specimens) and Site 3 (27 specimens) in Fig. 2.

The physicochemical parameters of the water on the investigated cave river did not vary between sampling sites and were the following: temperature: 12°C; conductivity: 3.18 µS/cm; dissolved oxygen: 10.66 mg/dm^3; biochemical oxygen demand over 5 days (BOD_5): 1.98; NO_3: <0.10 mg/dm^3; NH_4 concentration: 0.207 mg/dm^3; PO_3 concentration: 0.170 mg/dm^3. The granulometry varied among sites (Table 1). Sites 1 and 3 had a high organic content with moderately to poorly sorted fine sediments, while Sites 2 and 4 had lower organic content and more coarse sands. In addition to Gastrotricha in the examined material, we found protozoa (mainly Ciliata), nematodes and rotifers (Bdelloidea as well as Monogononta).

Table 3. DNA sequences of the gastrotrichs species used in phylogenetic analysis.

Species	GenBank acc. nos.		
	18S	**28S**	**COI**
Arenotus strixinoi	JQ798537	JQ798608	JQ798677
Aspidiophorus ophiodermus	JN185463	JN185510	–
Aspidiophorus polystictos	JQ798597	JQ798664	JQ798726
Aspidiophorus tetrachaetus	JN185505	JN185540	JN185576
Bifidochaetus arcticus	KP713403	KP713404	KP713405
Chaetonotus sp. Kånneby, Todaro & Jondelius, 2013	JQ798555	–	JQ798692
Chaetonotus sp. 1 Kånneby, Todaro & Jondelius, 2013	JQ798601	JQ798668	JQ798730
Chaetonotus (Chaetonotus) antrumus Kolicka sp. nov.	KX538804	KU705232	KU705230
Chaetonotus (Chaetonotus) daphnes	JQ798549	JQ798617	JQ798687
Chaetonotus (Chaetonotus) cf. *sphagnophilus*	JQ798604	JQ798671	JQ798733
Chaetonotus (Chaetonotus) cf. *laroides*	JQ798602	JQ798669	JQ798731
Chaetonotus (Chaetonotus) microchaetus	JQ798575	JQ798618	JQ798684
Chaetonotus (Chaetonotus) cf. *similis*	JQ798592	JQ798660	JQ798722
Chaetonotus (Chaetonotus) similis	JQ798578	JQ798648	JQ798710
Chaetonotus (Chaetonotus) polyspinosus	JQ798563	JQ798654	JQ798717
Chaetonotus (Chaetonotus) maximus 1	JQ798577	–	JQ798709
Chaetonotus (Chaetonotus) maximus 2	JQ798574	JQ798646	JQ798706
Chaetonotus (Primochaetus) armatus	JQ798594	–	JQ798723
Chaetonotus (Primochaetus) acanthocephalus	JQ798569	–	JQ798701
Chaetonotus (Primochaetus) acanthodes 1	JQ798544	JQ798616	JQ798682
Chaetonotus (Primochaetus) acanthodes 2	JQ798552	JQ798624	–
Chaetonotus (Primochaetus) heideri 1	JQ798547	JQ798619	JQ798685
Chaetonotus (Primochaetus) heideri 2	JQ798590	JQ798657	JQ798720
Chaetonotus (Hystricochaetonotus) hystrix 1	JQ798557	JQ798627	–
Chaetonotus (Hystricochaetonotus) hystrix 2	JQ798603	JQ798670	JQ798732
Chaetonotus (Hystricochaetonotus) cf. *novenarius*	JQ798566	JQ798636	JQ798699
Chaetonotus (Marinochaetus) mariae	JQ798558	JQ798628	–
Chaetonotus (Schizochaetonotus) dispar	JQ798561	JQ798631	JQ798696
Chaetonotus (Schizochaetonotus) neptuni 1	JQ798539	JQ798610	JQ798679
Chaetonotus (Schizochaetonotus) neptuni 2	JQ798595	JQ798662	JQ798724
Chaetonotus (Schizochaetonotus) schultzei	JQ798596	JQ798663	JQ798725
Chaetonotus (Wolterecka) uncinus	JQ798540	JQ798611	–
Chaetonotus (Zonochaeta) bisacer	JQ798565	JQ798635	–
Halichaetonotus euromarinus	JQ798551	JQ798623	–
Halichaetonotus sp. 1 Kånneby, Todaro & Jondelius, 2013	JQ798600	JQ798667	JQ798729
Halichaetonotus sp. 2 Kånneby, Todaro & Jondelius, 2013	JQ798560	JQ798630	JQ798695
Halichaetonotus aculifer	JQ798550	JQ798622	JQ798688
Halichaetonotus paradoxus	JQ798599	JQ798666	JQ798728
Heterolepidoderma loricatum	JQ798541	JQ798612	–
Heterolepidoderma macrops	JN185469	JN185515	JN185548
Heterolepidoderma ocellatum	JN185475	JN185519	JN185554
Heterolepidoderma sp.	JQ798554	–	JQ798691
Ichthydium (Furficulichthys) skandicum	JQ798573	JQ798645	JQ798705
Lepidochaetus brasilense 1	JN185458	JN185507	JQ798680
Lepidochaetus brasilense 2	JN185495	JQ798658	JN185568
Lepidochaetus zelinkai	JN185486	JN185527	JN185564
Lepidodermella intermedia	JN185468	JN185514	JN185547
Lepidodermella minor minor	JN185474	–	JN185553
Polymerurus nodicaudus 1	JN185460	–	JN185542
Polymerurus nodicaudus 2	JN185502	JN185537	JN185573
Polymerurus nodicaudus 3	JN185465	JN185512	JQ798689
Polymerurus nodicaudus 4	JN185473	JQ798642	JN185552
Polymerurus rhomboides 1	JQ798584	–	JQ798715
Polymerurus rhomboides 2	JN185467	JN185513	JN185546
Polymerurus rhomboides 3	JN185493	JN185533	JN185567

Taxonomic account

Phylum Gastrotricha Mečnikow, 1865
Order Chaetonotida Remane, 1925 [Rao & Clausen 1970]
Suborder Paucitubulatina d'Hondt, 1971
Family Chaetonotidae Gosse, 1864 (*sensu* Leasi & Todaro 2008)
Subfamily Chaetonotinae Gosse, 1864 (*sensu* Kisielewski 1991)

Genus ***Chaetonotus*** Ehrenberg, 1830

Type species

Chaetonotus larus (Müller, 1773).

Type area

Denmark.

Subgenus ***Chaetonotus*** *sensu stricto* Ehrenberg, 1830

Type species

Chaetonotus larus (Müller, 1773).

Type area

Denmark.

Chaetonotus (Chaetonotus) antrumus Kolicka sp. nov.
urn:lsid:zoobank.org:act:BF874601-C073-465F-B50B-48D73DB5A4C5
Figs 4–11; Table 4; Appendix

Diagnosis

Slender body, length from 91.2 to 129.7 µm. Head five-lobed, cephalion and pleuria weakly marked in the head outline. Hypostomium small and rhomboidal. Ocellar granules absent. Scales small, three-lobed and with strong keels. One pair of one-lobed, keeled scales on the dorsal side of the posterior part of the trunk, and on the dorsal and dorsolateral sides of the furcal appendages. Two pairs of three-lobed, spined scales present on the ventral side of the furcal appendages. Scales distributed in 29–35 total longitudinal rows (11–13D+6–8DL+6L+4–6LV+2V) with 23–27 scales in the central row, and differing morphologically in the areas of the head, neck and trunk, respectively. Spines thick, simple, with blunt ends. Spine lengths strongly vary: spines of the head are longer than those of the neck; spines of the neck are short, but become progressively longer to the widest body region, after which they gradually shorten towards the furcal base. The spines gradually increase in length from lateral to ventral body side towards the ciliary bands. Ventral scale spines longer than the others and hair-like. Last pair of parafurcal spines longer and stronger. Ventral interciliary field naked, except for the posterior trunk region. A pair of ventral terminal scales long, oval with shallow posterior notches, keeled and spineless. Pharynx narrow with two weakly marked dilatations. Straight intestine with a distinct, short anterior section appearing as a narrow band.

Etymology

From Latin '*antrum*', cave, referring to the habitat where the species was found.

Material examined

Holotype

MONTENEGRO: adult, Crnojevica River flowing in Obodska Cave, 42°21.118′ N, 19°0.304′ E, sample 3, sampling site 3, 29 Jul. 2015, Piotr Gadawski leg., determined by Małgorzata Kolicka (photomicrograph in the Natural History Collections, Adam Mickiewicz University, Poznan: NHC-GCCA-12-1-20/h).

Paratypes

MONTENEGRO: 31 adults, 2 subadults, 2 juveniles, Crnojevica River flowing in Obodska Cave, 42°21.118′ N, 19°0.304′ E, samples 1 and 3, sampling sites 1 and 3, 29 Jul. 2015, Piotr Gadawski leg., determined by Małgorzata Kolicka (Natural History Collections, Adam Mickiewicz University, Poznan under accesing number: NHC-GCCA-12-21-50).

Description

This new species has a slender body. Its head is wider than the neck and separated from the trunk by a distinct neck constriction. The neck extends into the trunk, which gradually widens towards its widest region beyond its midpoint (ca U61), after which it gradually tapers towards a distinct furcal base at U84. The branches of the furca are set wide apart. The furcal indentation is V-shaped, and the adhesive tubes diverge posteriorly. They measure 10.1–11.3 μm, are straight and thin and do not taper towards their blunt ends (Figs 4–6).

The head is five-lobed and semi-circular. All plates are visible in the dorsal head outline. The cephalion (U1–U5) adheres to the head along its entire length, is narrow and widens at the dorsal edge. The epipleuria (U4–U6) are small and slightly convex. The hypopleuria (U7–U13) are more than twice as large as the epipleuria. The hypopleuria are not visible from the dorsal side; only their outline is marked in body shape (Figs 4A, 7). The hypostomium (U5–U8) is short and rhomboidal with slightly rounded edges and a strong anterior edge (Fig. 4C). Two pairs of cephalic ciliary tufts are present. The anterior tufts have four cilia each that emerge from between the cephalion and epipleuria and are arranged in lines around the lateral edges of the cephalion. The beginning of these lines (the first two cilia) is clearly visible on the dorsal side. The anteriormost cilium in both anterior tufts is fairly short (the shortest). The second cilium is longer than the first. The third cilium is very long and is the longest of all cilia in the tuft. The posteriormost cilium is shorter than the third and similar in length to the second cilium. The posterior tufts have five cilia each and emerge ventrally at the anterior edge of the hypopleuria. The length of the cephalic cilia in the posterior tufts increases from the anteriormost to the fourth cilium. The posteriormost cilium is similar in length to the first (see Appendix). Ocellar granules are not present. The mouth ring is narrow, located sub-terminally at U2–U3 and has weakly marked, granular reinforcements. Short inner hairs are present inside the mouth ring and suboral hairs are located around it.

The body is covered by small, three-lobed scales and single one-lobed scales that adhere over their entire surface to the cuticle (Figs 5–9). Scales are distributed in 29–35 total longitudinal and alternating rows (11–13D+6–8DL+6L+4–6LV+2V) with 23–27 scales in the dorsal central row. Each scale has a strong keel and triangular with a deeply-notched posterior edge. On the head, neck and anterior and middle parts of the trunk, the longitudinal rows of scales run parallel to each other, while in the posterior part of the trunk and on the furcal base the scales gradually converge towards the central longitudinal row (Figs 4, 7–9). The scales on the head, neck and trunk are arranged close to one another, but their edges do not adhere or overlap. The longitudinal rows of scales begin on the head beyond the posterior edges of the cephalion, epipleuria and hypopleuria. The scales show a strong morphological diversity in postero-lateral lobe distinctness, edge roundness and size throughout the different surfaces of the head, neck and trunk regions. On the head, there are deeply-notched, rounded, wide triangles with rounded postero-lateral lobes that are weakly differentiated from the central lobe. On the neck, scales are narrower, and

their postero-lateral lobes show a weaker separation from the central lobe (see Appendix; Figs 4A, 5). On the trunk, scales are shaped like narrow, deeply-notched triangles with their postero-lateral lobes clearly differentiated from the central lobe and with edges that are less rounded (Figs 4–5, 8A, C, E, 9A). The size of the scales decreases rapidly at the beginning of the neck, after which it gradually increases towards the beginning of the trunk (head: 1.6–3.8 µm length × 1.8–4.3 µm width vs neck: 1.3–3.3 µm length × 1.4–3.9 µm width vs trunk: 2.5–5.6 µm length × 1.6–4.3 µm width). The dorsal head and neck scales differ most from one another (Figs 4A, 5, 7A), whereas in the other areas of the head and neck, the differences in shape and size between the scales are gradual. The size of the scales of the trunk increases from the anterior end towards the widest trunk region, after which it decreases towards the furcal base (see Appendix). On the posterior part of the trunk, scales are clearly smaller than those at the widest point of the body. A fine (1.9–2.7 µm length × 1.3–1.8 µm width) one-lobed, keeled and spineless scale is located at U78 on the dorsal part of the trunk, anterior to each scale bearing a sensory bristle (Figs 4A, 8C) and is shaped like a strongly-rounded triangle. Medially, on the dorsal side of the furcal appendages (U86–U88), three three-lobed scales are present that are slightly narrower than the other scales of the trunk (see Appendix; Figs 4A, 8G). Lateral to these scales, on the furcal appendages (U85–U88), there are two pairs of elongated one-lobed scales shaped like narrow ovals with a weakly-notched posterior edge. The anterior one of each pair of scales is located dorsally, has a strong keel and a long, straight spine, whereas the posterior one is located dorsolaterally and has a long keel, but no spine. The lateral edges of these scales are partially overlapping. On the lateral side of the furcal appendages (U86–U90), two pairs of three-lobed scales, of the same type as the scales of the trunk, with spines are present (Figs 6, 9A). The dorsal, dorsolateral, lateral, ventrolateral and ventral scales do not strongly vary in size, except that the scales in the area of the neck and in the longitudinal rows next to the ciliary bands are considerably smaller than the others. The ventral scales of the longitudinal rows located closest to the ventral ciliary bands are about half the size of the scales in the other rows (head: 1.6–2.9 µm length × 1.8–2.3 µm width; neck: 1.3–1.8 µm length × 1.4–2.0 µm width; trunk: 2.5–3.0 µm length × 1.6–2.0 µm width) and have their central lobe rotated about 20° towards the bands (see Appendix; Figs 4C, 8C, 10C).

The spines arising from the posterior scales region are thick and straight, taper very slightly towards their blunt ends and have no lateral denticles (Figs 4, 7B, D, 8B, D, F, 9B, 10E). The spines that adhere directly to the cephalion and pleuria are the shortest of the head spines (Fig. 7B). The spines on the head increase in length (1.1–3.1 µm), whereas those on the neck decrease rapidly in length. The spines on the neck are much shorter than those in the head area; the spines are merely vestigial halfway down the neck, after which they gradually lengthen towards the trunk (0.5–2.7 µm) (Figs 4, 7B). The spines on the trunk gradually and slightly lengthen from the beginning of the trunk (ca U30) up to the widest body region (ca U61), after which they gradually shorten towards the furcal base at U84 (1.3–4.1 µm) (Figs 4, 8B, D, F). The pair of posteriormost lateral trunk spines is slightly longer and thicker than the surrounding spines (3.4–5.9 µm). Parafurcal spines emerging from two lateral scales per side on the furcal appendages are slightly thicker and longer than the other spines of the body, the posteriormost pair is longer, thicker and stronger than those of the preceding pair (see Appendix; Fig. 4). These spines taper slightly towards their blunt distal ends. The dorsal and dorsolateral spines do not vary substantially in length (Table 4). The spines lengthen gradually and slightly from the lateral side towards the ciliary bands (Fig. 9B). The spines arising from the ventral longitudinal row of scales located closest to the ciliary bands are much longer than those of the body, curved, and hair-like along their entire length (head: 5.1–8.6 µm; neck: 5.0–9.0 µm; trunk: 7.1–14.0 µm).

This species has three pairs of dorsal sensory bristles (Fig. 4). The first pair is located on the head, directly posterior to the cephalion, near the lateral edges of the epipleuria (U5), and each bristle emerges from a small, round papilla. The second pair is located on the neck (U25) and each bristle emerges from a small, rounded papilla. The third, posterior pair, which emerges from double-keeled scales located in

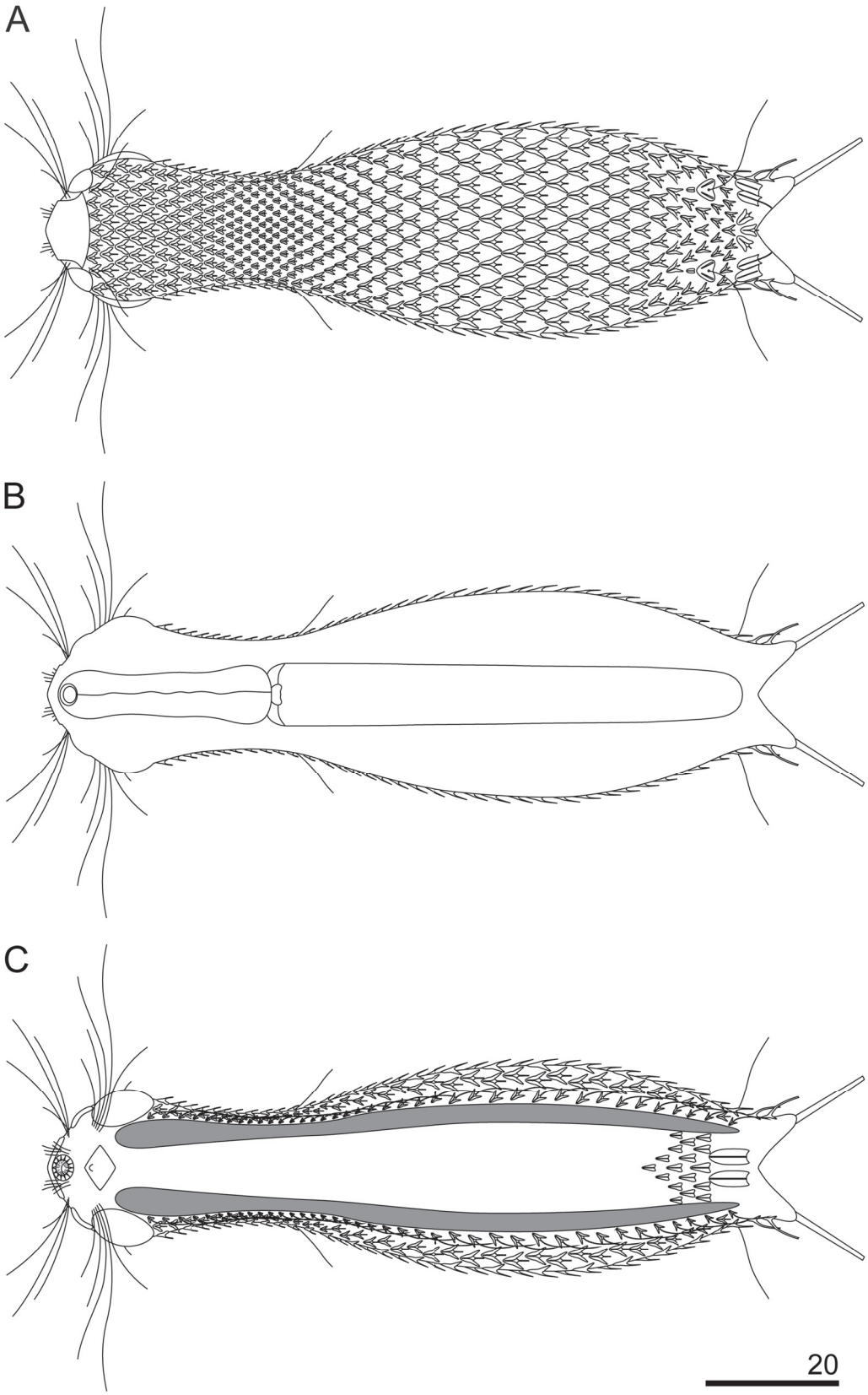

Fig. 4. *Chaetonotus (Chaetonotus) antrumus* Kolicka sp. nov., schematic drawings. **A**. Dorsal body view. **B**. Internal body view. **C**. Ventral body view.

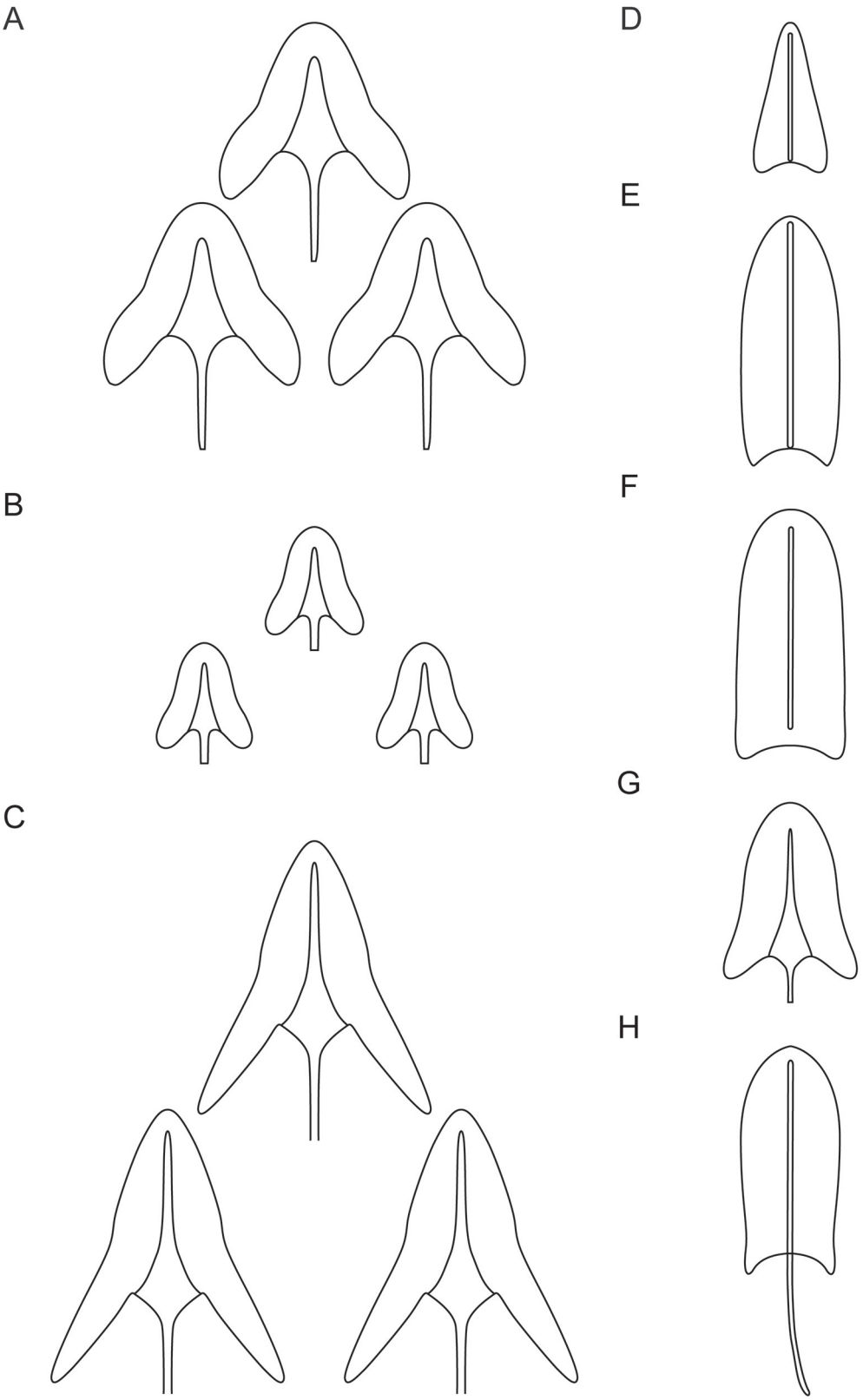

Fig. 5. *Chaetonotus (Chaetonotus) antrumus* Kolicka sp. nov., schematic drawings of the scales. **A**. Head region scales. **B**. Neck region scales. **C**. Trunk region scales. **D**. Ventral interciliary field scales. **E**. Posteriormost ventral field scales. **F**, **H**. Furcal appendages dorsolateral one–lobed scales. **G**. Furcal appendages dorsal three-lobed scales.

the posterior part of the trunk (U79–U80), is shaped like deeply-notched triangles with unconnected keels (Figs 4A, 5).

On the ventral side, the longitudinal ciliary bands begin at U8 and run back to U84 (Fig. 4C). They are wider in the area of the head than in the other parts of the body. Most of the ventral interciliary field is naked: fine, keeled, spined scales are present only in the posterior part of the trunk (from ca U78 to U82) (Figs 4C, 8H). Their differentiation increases towards the posterior body region: the anterior scales are weakly delineated and partially submerged in the cuticle. These scales are shaped like narrow triangles with a very weakly notched posterior edge. The scales of the ventral interciliary field increase in size towards the posterior end of the body (1.4–3.7 μm length × 1.1–1.9 μm width). The terminal scales are located at U82–U85 and are shaped like long, narrow ovals with a very weakly notched posterior edge and have a long keel running along their entire length, but are spineless (Figs 4C, 5E).

The pharynx (U2–U28) is relatively narrow and has weak anterior and posterior dilatations, with the posterior dilatation wider than the anterior one (Figs 4B, 7C; Appendix). The pharynx connects through the small and narrow pharyngeal intestinal junction (U30) to a straight intestine (running from U29 to U86). The intestine has a distinct, short (U29–U31) anterior section marked as a narrow band (Fig. 4B).

Remarks

Chaetonotus (Chaetonotus) antrumus sp. nov. is an interstitial species which was recorded in the lotic system in a cave. The gastrotrich fauna in interstitial freshwater habitats is relatively rich, but composed

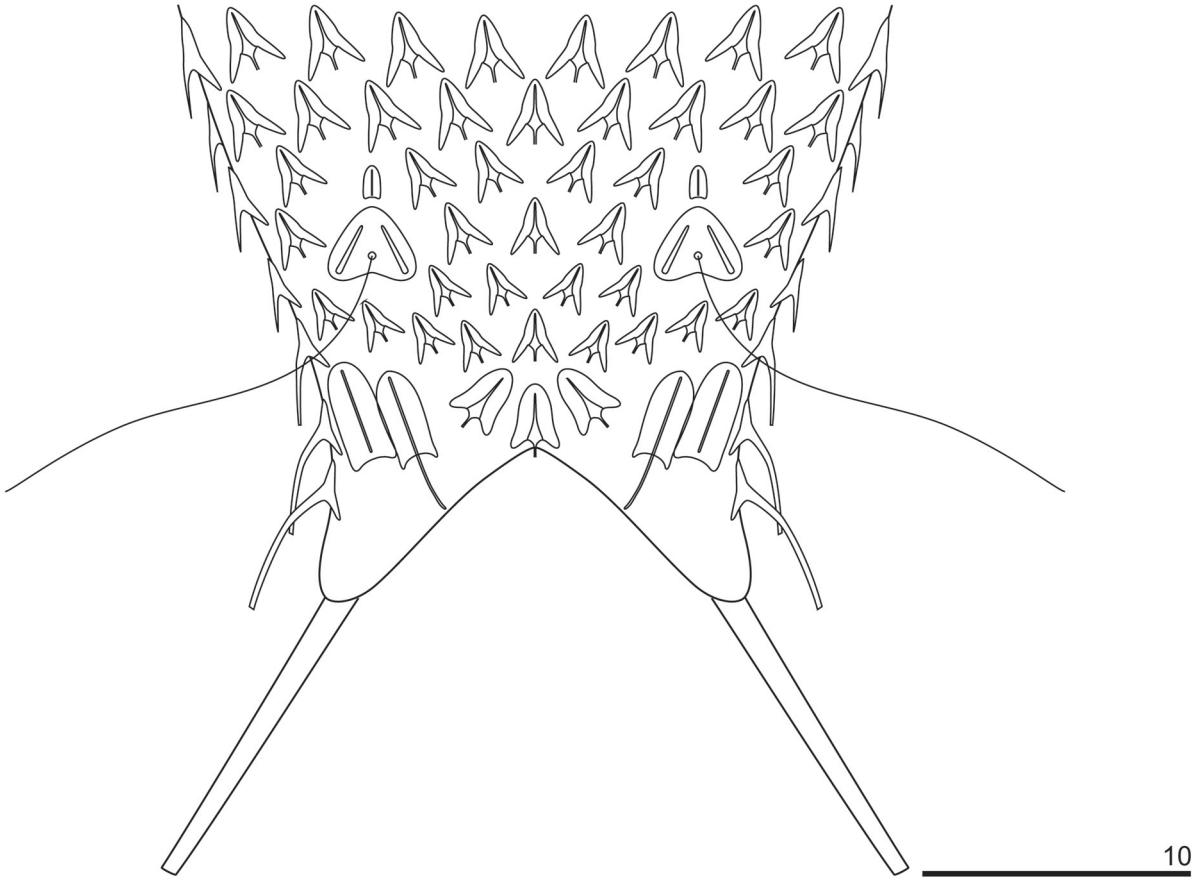

Fig. 6. *Chaetonotus (Chaetonotus) antrumus* Kolicka sp. nov., schematic drawings of the posterior trunk region, furcal base and furcal appendages.

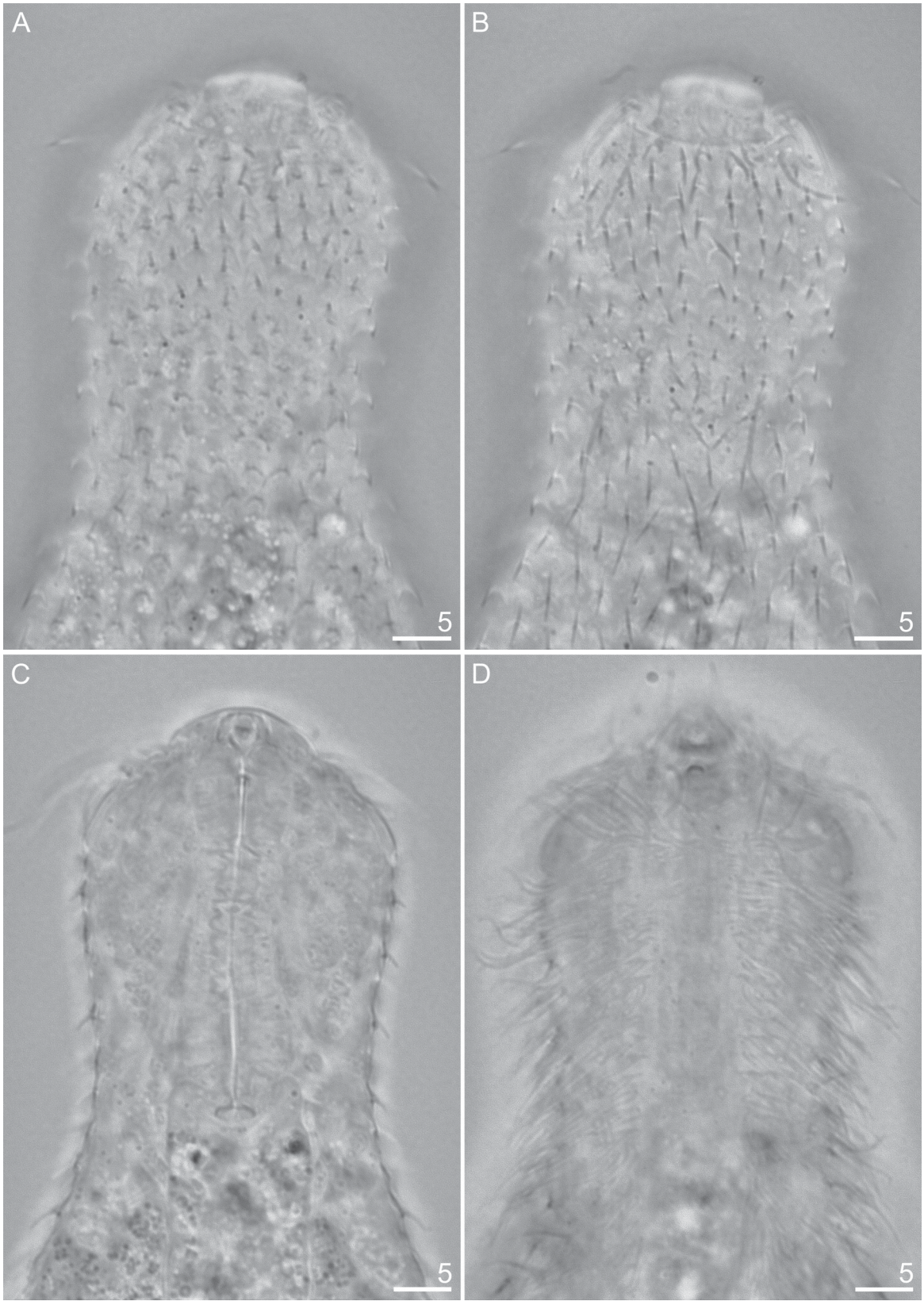

Fig. 7. *Chaetonotus (Chaetonotus) antrumus* Kolicka sp. nov. **A**. Dorsal view of scales on head and neck. **B**. Dorsal view of spines on head and neck. **C**. Internal view of head and neck. **D**. Head and neck, ventral view. (Bright field microphotographs.)

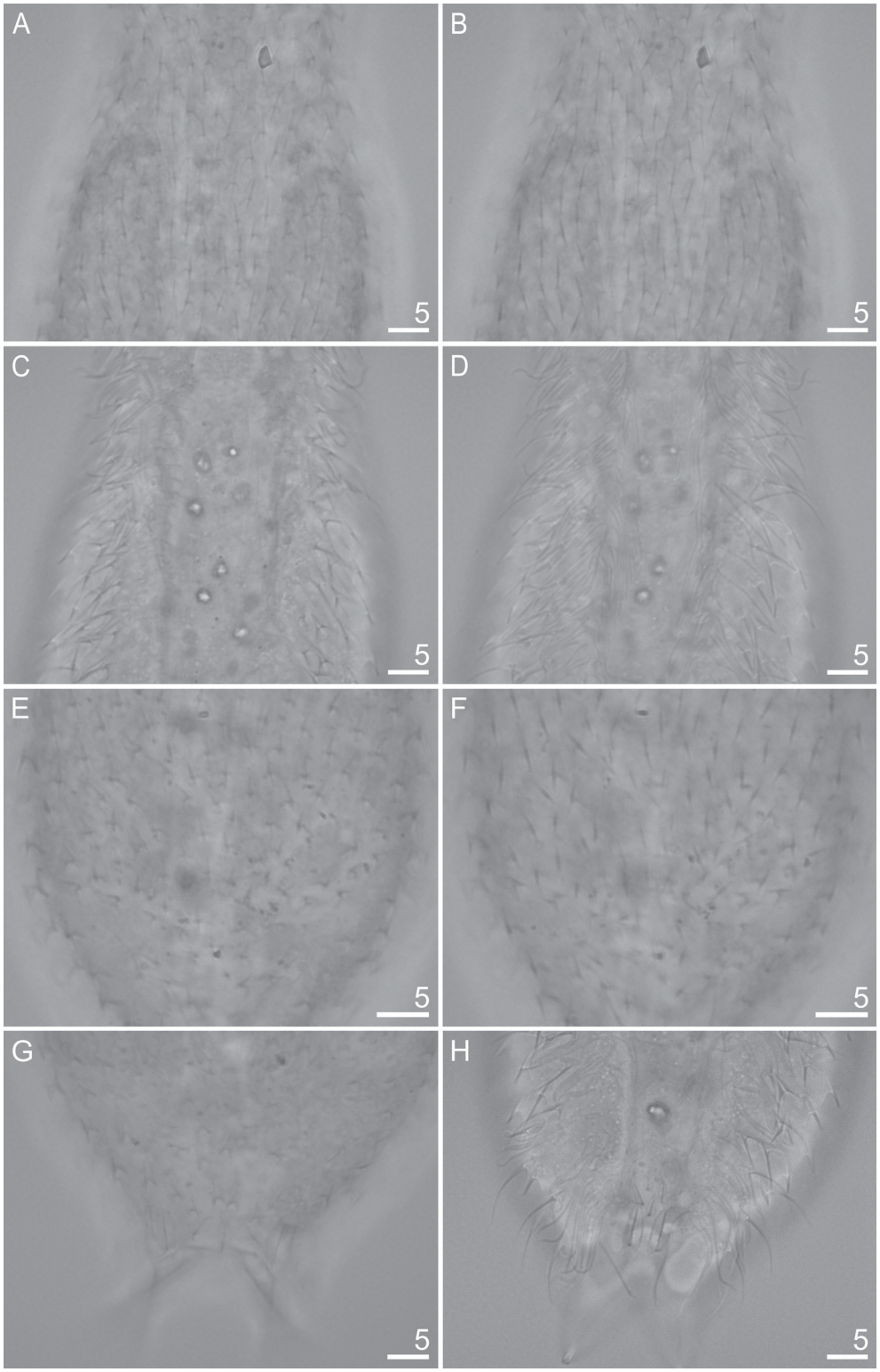

Fig. 8. *Chaetonotus (Chaetonotus) antrumus* Kolicka sp. nov., bright field microphotographs. **A**. Dorsal view of scales on trunk region. **B**. Dorsal view of spines on trunk region. **C**. Ventral view of scales on trunk region. **D**. Ventral view of spines on trunk region. **E**. Dorsal view of scales on posterior trunk region. **F**. Dorsal view of spines on posterior trunk region. **G**. Dorsal view of scales on furcal base and furcal appendages. **H**. Ventral view of posterior trunk region with visible interciliary field scales and posteriormost interciliary field scales.

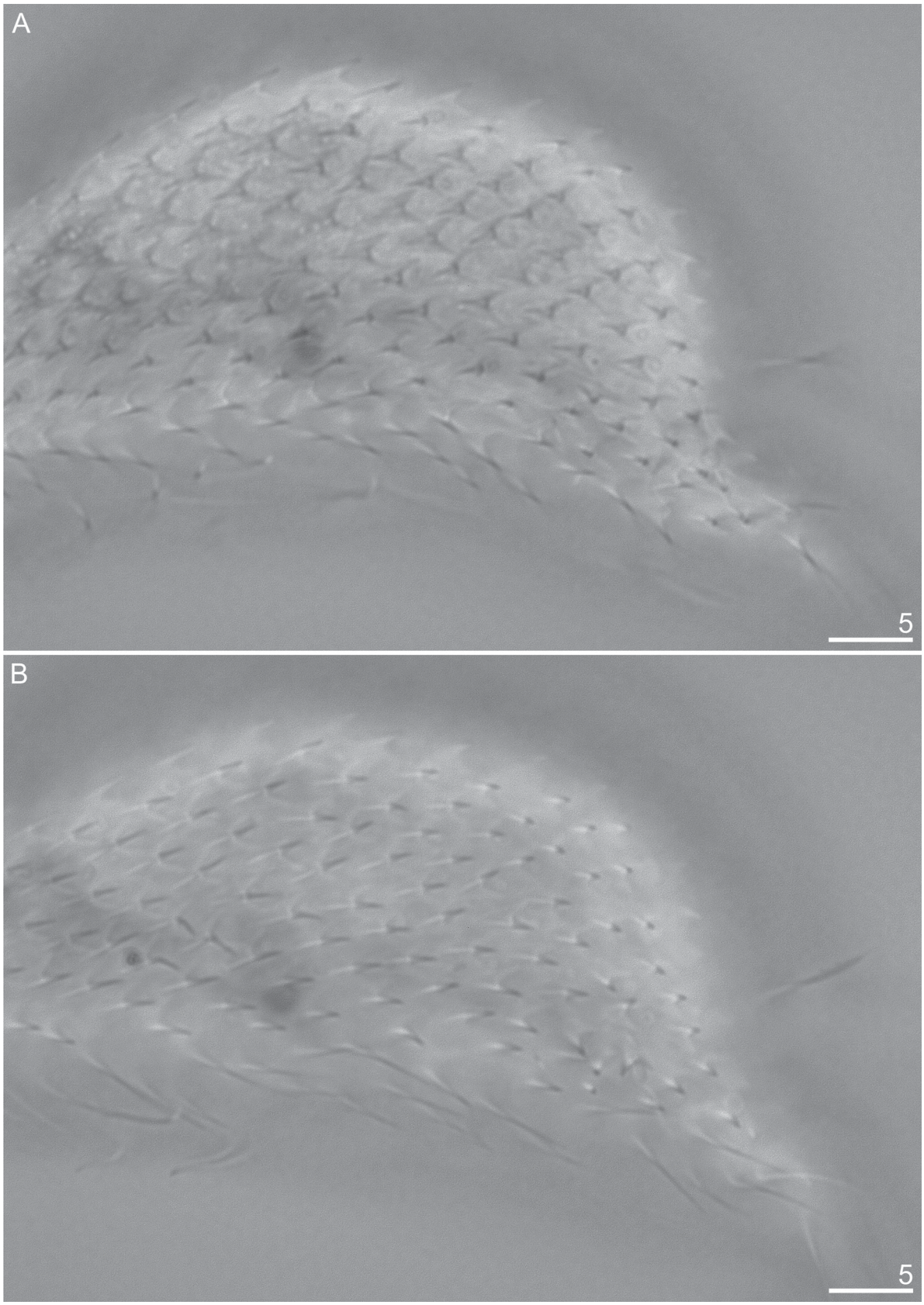

Fig. 9. *Chaetonotus (Chaetonotus) antrumus* Kolicka sp. nov., bright field microphotographs. **A**. Lateral view of scales on trunk. **B**. Lateral view of spines on trunk.

Table 4. Condensed comparison of the most important differential characters between species most similar to *Chaetonotus (Chaetonotus) antrumus* Kolicka sp. nov. Measurements are given in micrometers (µm).

Character	***C. (C.) antrumus*** Kolicka sp. nov.	***C. (C.) naiadis*** Balsamo & Todaro, 1995	***C. (C.) daphnes*** Balsamo & Todaro, 1995
Body length	119.1–129.7	89.0–140.0	141.0–173.0
Cephalic pleuria	Cephalion narrow, extended dorsally; epipleuria small visible from the dorsal body side; hypopleuria large not visible from dorsal body side. Hypostomium present	Cephalion wide; epipleuria large; hypopleuria small; clearly visible from the dorsal body side. Hypostomium present	Cephalion wide; epipleuria large, clearly visible on the dorsal body side; hypopleuria smallpresent only on the ventral body side. Hypostomium absent
Place of arising cephalic cilia	Anterior tufts: in lines between cephalion and epipleuria; posterior tufts: at the anterior edge of the hypopleuria on the ventral side	Anterior and posterior tufts: lateral	Anterior tufts: dorsally at the head top; posterior: dorsally
Pharynx length	31.9–34.9	26.0–33.0	36.0–44.0
Anterior intestinal section morphologically different	Present	Absent	Absent
Furca length	19.8–23.2	12.0–17.0	14.0–20.0
Adhesive tube length	10.1–11.3	9.0	7.0–11.0
Type of furca indentation	V-shaped	V-shaped	Helmet-shaped
Number of scales in single longitudinal row	24–27	20	25–33
Total number of longitudinal alternating rows of scales	29–35	23–31	45–53
Type of scales	Almost all three-lobed with strong keels and straight spines; shape strongly differentiated within body regions	One-lobed with strong keels and straight spines; shape undifferentiated within body regions	One-lobed with strong keels and straight spines; shape undifferentiated within body regions
Size of scales	Small; size strongly differentiated within body regions	Small; size slightly increasing posteriorly	Small; similar size all over the body
Presence of scales with two keels and two spines on the furcal appendages	Absent	One pair of scales with two keels and two spines present dorsolateraly	Absent
Scale coverage of the ventral interciliary field	Only the posterior end of the trunk covered by scales	Only the posterior end of the trunk covered by scales	Entire ventral interciliary field covered by scales
Type of terminal scales of the ventral interciliary field	Oval with shallow posterior notches, keeled, spineless	Oval without posterior notches, keeled, spined	Oval without posterior notches, keeled, spineless
Variety of spines length	Strongly differentiated length of spines on the head, neck (short, vestigial on dorsal area) and trunk; length of the spines gradually lengthen from the lateral to the ventral sides of the body; much longer spines on the ventral body sides	Similar length of spines on the dorsal, dorsolateral, lateral sides of the head, neck and trunk; much longer spines on the ventrolateral body sides	All spines similar length
Type of posteriormost pair of the lateral trunk spines	Slightly longer and thicker than surrounding spines	Same as other spines	Same as other spines
Type of last pair of the parafurcal spines	Longer, thicker and stronger than other spines	Same as other spines	Same as other spines
Number of dorsal sensory bristles	3 pairs	2 pairs	2 pairs

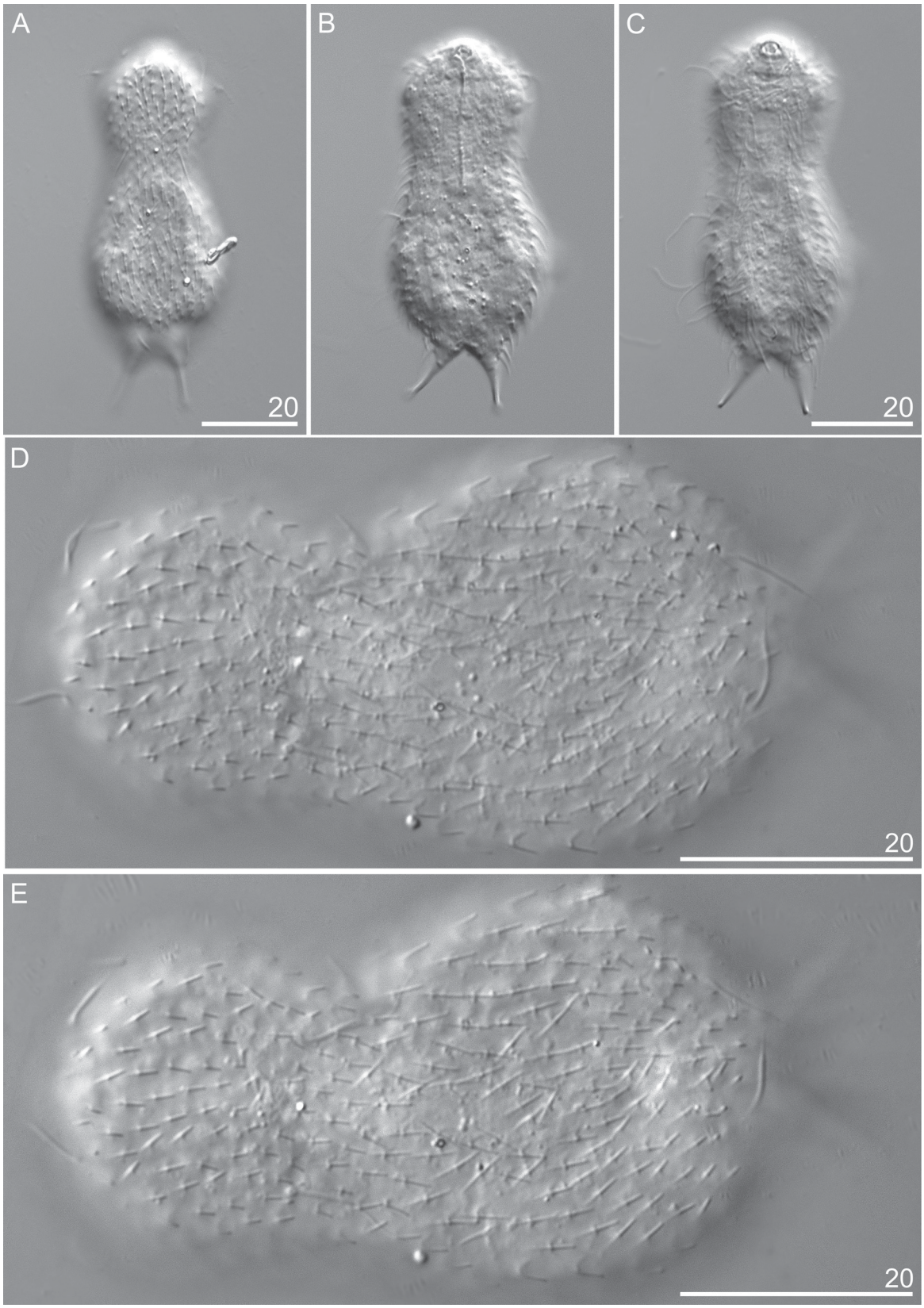

Fig. 10. *Chaetonotus (Chaetonotus) antrumus* Kolicka sp. nov., juvenile specimen, differential interference contrast microphotographs. **A**. Body, dorsal view. **B**. Body, internal view. **C**. Ventral body view. **D**. Dorsal view of scales. **E**. Dorsal view of spines.

of fewer species than in epibenthic or periphytic habitats (e.g., Balsamo *et al.* 2015). Interstitial communities are composed of not only taxa specific to them, but also of eurytopic species. Out of ca 40 species found in sandy biotopes, fewer than 10 seem to constitute exclusively interstitial taxa (Balsamo *et al.* 2015). All of the species share certain morphological traits, e.g., a small body size, a poorly ornamented cuticular covering, a well developed locomotory ciliature and adhesive organs (Balsamo & Fregni 1995; Balsamo *et al.* 2015). Entire sets of these characteristics also occur in *C. (C.) antrumus* sp. nov.

Usually, one or two pairs of sensory bristles have been described in Chaetonotidae, but in *C. (C.) antrumus* sp. nov., three pairs of dorsal sensory bristles are present. The presence of dorsal sensory bristles in the area of the head has previously been noted in only two species of *Chaetonotus*: *C. (C.) brevispinosus* Zelinka, 1889 and *C. (C.) sanctipauli* Kisielewski, 1991. Perhaps three pairs of dorsal sensory bristles occur more frequently in Chaetonotidae; the location of the first pair of dorsal sensory bristles on the head near the cephalion and the cephalic cilia, however, may have led to these sensory bristles being

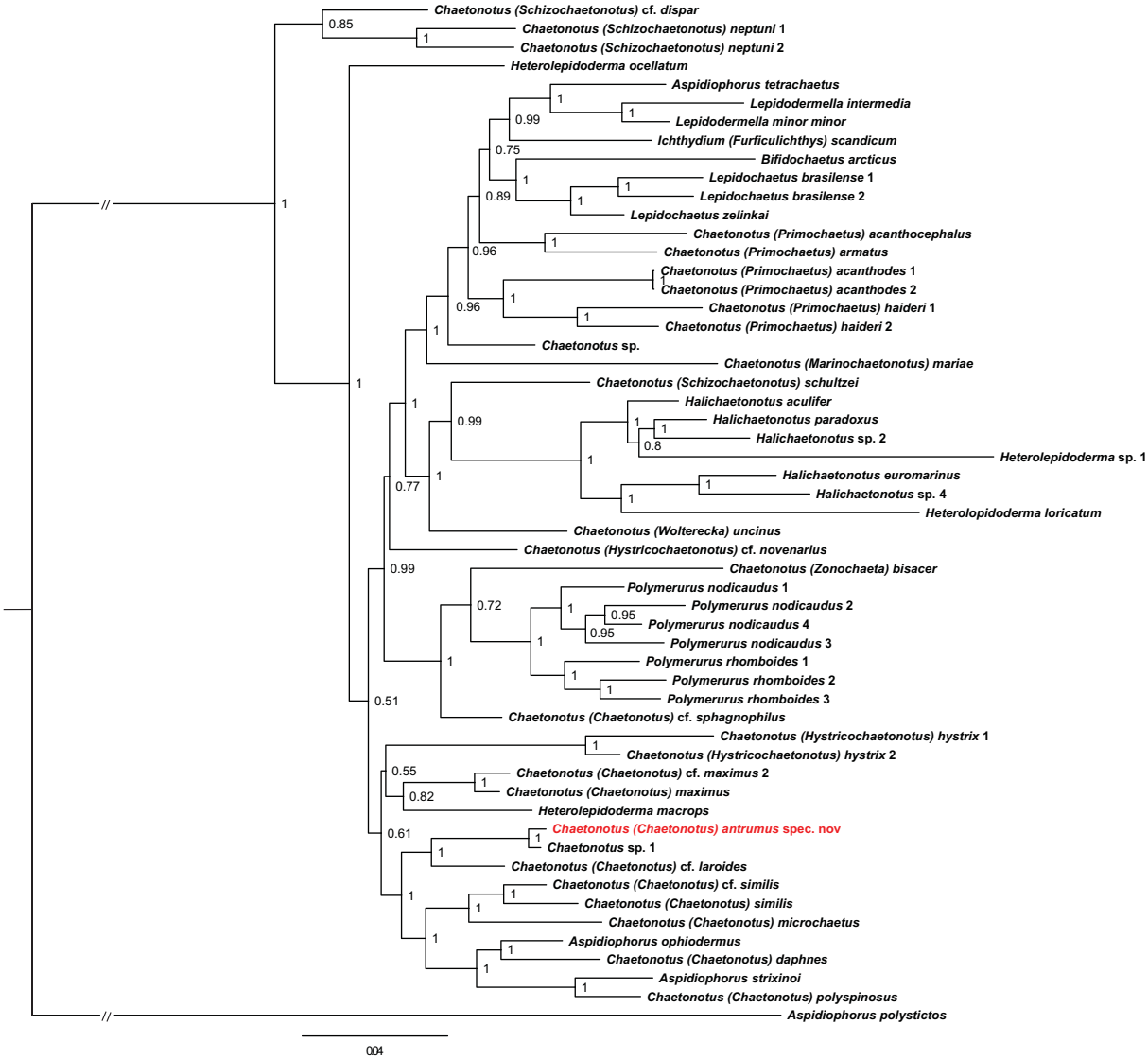

Fig. 11. Phylogenetic relationships of Chaetonotidae inferred from the Bayesian analysis of 18S rRNA, 28S rRNA and COI sequence data (for details on the species names see Table 3).

obscured by the cilia or erroneously interpreted as one of the cilia. Thus, the presence of dorsal sensory bristles on the head cannot be considered as a good diagnostic characters at the species level.

The presence of a developing egg was observed in 21 out of 32 adult specimens of *C. (C.) antrumus* sp. nov. However, sperm and an X-organ were not observed.

Chaetonotus (Chaetonotus) antrumus sp. nov. showed very quick locomotion under microscopic observation. The species often remained in motion even after its integument had burst from compression under a cover glass, thus producing a visible deformation.

Sequence diversity and phylogenetic relationships

The COI alignment for the distance calculations comprised 628 bp of unambiguous sequence data for three specimens of *Chaetonotus (Chaetonotus) antrumus* sp. nov. We found two haplotypes that differed in eight nucleotide positions (K2P = 0.013; SD = 0.005). All substitutions were located at synonymous sites, i.e., both haplotypes coded for the same amino acid sequence. The nuclear data, including 4809-bp of the DNA region coding for 18S rRNA, ITS1, 5.8S, ITS2, and 28S rRNA, showed no intraspecific variation. All sequences are deposited in GenBank under accession numbers KU705230, KU705231 (COI); KX538804 (18S); KU705232 (28S); KU705233 (ITS).

A phylogenetic analysis (Fig. 11) recovered, with maximum support, *C. (C.) antrumus* sp. nov. as closely related to the undetermined *Chaetonotus* sp. 1 TK-2012 (Kånneby *et al.* 2013); both grouped with *C. (C.)* cf. *laroides.* This clade was in a sister relation to a clade consisting of some representatives of *Chaetonotus (Chaetonotus)* Ehrenberg, 1830 and *Aspidiophorus* (Voigt, 1903) and including *Chatonotus (Chaetonotus) daphnes* Balsamo & Todaro, 1995, which is morphologically most similar to the new species.

Differential diagnosis

Even if the new species was recorded from a sandy habitat, it is not similar to any other species considered as exclusively interstitial taxa. *Chaetonotus* Ehrenberg, 1830 is a polyphyletic genus, containing varied species. Of all the 165 currently known nominal freshwater representatives of this genus, *C.(C.) antrumus* sp. nov. is morphologically closest to *C. (C.) naiadis* Balsamo & Todaro, 1995 and *C. (C.) daphnes* Balsamo & Todaro, 1995, both of which were originally reported from Italian mountain pools. These two species were selected from all the *Chaetonotus* representatives for the comparison of the new species due to a similarity in terms of (1) the alignment of scales whose edges are juxtaposed; the presence of a different type of scales on the dorsal and dorsolateral sides of the furcal base; (2) the type of scales on the ventral interciliary field; (3) the number of terminal scales of the ventral interciliary field; (4) two longitudinal bands of ventral locomotor cilia wider on the head region. Despite the fact that from all of the hitherto known species, *C. (C.) naiadis* and *C. (C.) daphnes* have the highest number of common features with the newly described species, they are significantly different from *C. (C.) antrumus* sp. nov., most strikingly in the scale type and shape. All the differences between the new species and the most morphologically similar taxa have been summarized in Table 4.

Discussion

The presence of *Chaetonotus (Chaetonotus) antrumus* sp. nov. in only two of four sampling sites may reflect the habitat selectivity by the species. The species was observed only in the samples with a high organic matter content, a minimum diameter spectra of the sand grain, and moderately to poorly sorted sediments. This result confirms previous observations regarding the habitat preferences of many freshwater gastrotrichs, which appear to prefer finer sediments with high organic matter content (e.g., Kisielewski 1997; Balsamo & Todaro 2002; Balsamo *et al.* 2014). However, the occurrence and

composition of the Gastrotricha fauna inhabiting caves may depend not only on the physicochemical habitat properties (temperature, sunlight, granulometry of the sediments, the water flow rate) (e.g., Balsamo *et al.* 2014), but also on the possibility of colonization and food availability. Gastrotrichs, as other meiobenthic invertebrates, have limited locomotory abilities. Dispersal in freshwater gastrotrichs is probably limited to migration through aquatic sediments and dispersal of resistant eggs (see below).

The result of our molecular phylogenetic analysis is for the greater part congruent with the previous molecular phylogenies of Chaetonotidae (Kånneby *et al.* 2013; Kolicka *et al.* 2016) and gave further evidence to the high degree of polyphyletism of chaetonotid genera. Freshwater species of the order Chaetonotida, which may produce opsiblastic, resting eggs, are known for passive migration with water currents, watercourses, surface run-offs, wind and being carried by more mobile animals, e.g., birds, bats, amphibians, insects or annelids (e.g., Gerlach 1977; Kolicka *et al.* 2014). One of those vectors was most probably responsible for the transport of gastrotrichs into Obodska Cave. Because of their wide range of ecological tolerance and parthenogenetic reproduction, Gastrotricha may have persisted there and developed a population. When analyzing the fauna of cave ecosystems, it must be remembered that those habitats are not influenced by sunlight. Thus, there are no photoautotrophs and the ecosystem is based mainly on the influx of organic matter from outside the cave. Most of the currently known species of Gastrotricha feed on bacteria, detritus, and small algae (e.g., Bennett 1979; Balsamo & Todaro 2002; Todaro & Hummon 2008). The lack of unicellular autotrophs may not be a limiting factor for the majority of Gastrotricha species that feed mainly on bacteria (e.g., Balsamo *et al.* 2014).

Further studies will show whether *Chaetonotus (Chaetonotus) antrumus* sp. nov. is endemic to Obodska Cave, or more widely distributed and not associated with only one specific type of environment. The application of methods typical for integrative taxonomy (i.e., combined morphological, morphometric and molecular analyses), will allow verification of future reports regarding the presence of this species and accurate determination of its biogeography.

Acknowledgements

We would like to thank James Kirk for his invaluable comments on the draft version of the manuscript. The authors wish to thank two anonymous reviewers for their helpful comments. Special thanks to Małgorzata Kuźnik for figures of the new species used in this paper. Last but not least, we are grateful to Lech Kotwicki for help with the granulometric analysis, to Krzysztof Pabis for his helpful advise to this paper, and to Katarzyna Gadawska, Aleksandra Bańkowska, Magdalena Kłosowska, Grzegorz Michoński and Przemysław Śmietana for their help during the research expedition.

References

Balsamo M. & Fregni E. 1995. Gastrotrichs from interstitial fresh water, with a description of four new species. *Hydrobiologia* 302: 163–175. https://doi.org/10.1007/BF00027040

Balsamo M. & Todaro M.A. 2002. Gastrotricha. *In*: Rundle S.D., Robertson A.L. & Schmid-Araya J.M. (eds) *Freshwater Meiofauna: Biology and Ecology*: 45–61. Backhuys Publishers, Leiden.

Balsamo M., Grilli P., Guidi L. & d'Hondt J.-L. 2014. Gastrotricha: biology, ecology and systematics: families Dasydytidae, Dichaeturidae, Neogosseidae, Proichthydiidae. *In*: Dumont H.J.F. (ed.) *Identification Guides to the Plankton and Benthos of Inland Waters* 24. Backhuys Publishers and Margraf Publishers, Weikersheim.

Balsamo M., d'Hondt J.-L., Kisielewski J. & Pierboni L. 2008. Global diversity of gastrotrichs (Gastrotricha) in fresh waters. *Hydrobiologia* 595: 85–91. https://doi.org/10.1007/978-1-4020-8259-7_10

Balsamo M., d'Hondt J.-L., Kisielewski J., Todaro M.A., Tongiorgi P., Guidi L., Grilli P. & de Jong Y. 2015. Fauna Europea: Gastrotricha. *Biodiversity Data Journal* 3: e5800. https://doi.org/10.3897/BDJ.3.e5800

Balsamo M., d'Hondt J.-L., Pierboni L. & Grilli P. 2009. Taxonomic and nomenclatural notes on freshwater Gastrotricha. *Zootaxa* 2158: 1–19.

Bennett L.W. 1979. Experimental analysis of the trophic ecology of *Lepidodermella squamata* (Gastrotricha: Chaetonotida) in mixed culture. *Transactions of the American Microscopy Society* 98: 254–260.

Blott S. & Pye K. 2001. Gradistat: a grain size distribution and statistics package for the analysis of unconsolidated sediments. *Earth Surface Processes and Landforms* 26: 1237–1248. https://doi.org/10.1002/esp.261

Bonada N., Rieradevall M., Dallas H., Davis J., Day J., Figueroa R., Resh V.H. & Prat N. 2008. Multi-scale assessment of macroinvertebrate richness and composition in Mediterranean-climate rivers. *Freshwater Biology* 53: 772–788. https://doi.org/10.1111/j.1365-2427.2007.01940.x

Buchanan J.B. 1984. Sediment analysis. *In*: Holme N.A. & McIntyre A.D. (eds) *Methods for the Study of Marine Benthos*: 41–65. Blackwell Scientific Publications, Boston, MA.

Dabert J., Ehrnsberger R. & Dabert M. 2008. *Glaucalges tytonis* sp. nov. (Analgoidea: Xolalgidae) from the barn owl *Tyto alba* (Strigiformes: Tytonidae): compiling morphology with DNA barcode data for taxa descriptions in mites (Acari). *Zootaxa* 1719: 41–52.

Dabert M., Proctor H.C. & Dabert J. 2016. Higher-level molecular phylogeny of the water mites (Acariformes: Prostigmata: Parasitengonina: Hydrachnidiae). *Molecular Phylogenetics and Evolution* 101: 75–90. https://doi.org/10.1016/j.ympev.2016.05.004

Dabert M., Witalinski W., Kaźmierski A., Olszanowski Z. & Dabert J. 2010. Molecular phylogeny of acariform mites (Acari, Arachnida): strong conflict between phylogenetic signal and long branch attraction artifacts. *Molecular Phylogenetics and Evolution* 56: 222–241. https://doi.org/10.1016/j.ympev.2009.12.020

Danovaro R. 1996. Detritus-bacteria-meiofauna interactions in a seagrass bed (*Posidonia oceanica*) of the NW Mediterranean. *Marine Biology* 127: 1–13. https://doi.org/10.1007/BF00993638

Danovaro R., Corinaldesi C., Filippini M., Fischer U.R., Gessner M.O., Jacquet S., Magagnini M. & Velimirov B. 2008. Viriobenthos in freshwater and marine sediments: a review. *Freshwater Biology* 53: 1186–1213. https://doi.org/10.1111/j.1365-2427.2008.01961.x

Danovaro R., Luna G.M., Dell' Anno A. & Pietrangeli B. 2007. Measuring species richness based on microbial community fingerprints: the emperor has no clothes. *Applied and Environmental Microbiology* 73: 2399–2401. https://doi.org/10.1128/AEM.02383-06

d'Hondt J.-L. 1971. Gastrotricha. *In*: Barnes H. (ed.) *Oceanography and Marine Biology: an Annual Review* 9: 141–192. George Allen and Unwin Ltd, London.

Dinić J.B. 1965. *Crnojevićka Pecina, in Nase Jame.* Bohinec V. & Savnik R. (eds), Ljubljana.

Doderović M., Bulić Z. & Mijanović D. 2013. *Turistička valorizacija speološkog potencijala cetinjske subregije tourist valorization of caving in Cetinje.* Ćlovjek I krś 2014, Sarajevo.

Folk R.L. & Ward W.C. 1957. Brazos River bar: a study in the significance of grain size parameters. *Journal of Sedimentary Research* 27: 3–26. https://doi.org/10.1306/74D70646-2B21-11D7-8648000102C1865D

Fraschetti S., Gambi C., Giangrande A., Musco L., Terlizzi A. & Danovaro R. 2006. Structural and functional response of meiofauna rocky assemblages exposed to sewage pollution. *Marine Pollution Bulletin* 52: 540–548. https://doi.org/10.1016/j.marpolbul.2005.10.001

Gerlach S. 1977. Means of meiofauna dispersal. *Mikrofauna Meeresboden* 61: 89–103.

Giere O. 2009. *Meiobenthology. The Microscopic Fauna in Aquatic Sediments*. Springer Verlag, Berlin.

Goldman N. & Yang Z. 1994. A codon-based model of nucleotide substitution for protein-coding DNA sequences. *Molecular Biology and Evolution* 11: 725–736.

Hou Z. & Sket B. 2015. A review of Gammaridae (Crustacea: Amphipoda): the family extent, its evolutionary history, and taxonomic redefinition of genera. *Zoological Journal of the Linnean Society* 176 (2): 323–348. https://doi.org/10.1111/zoj.12318

Hummon W.D., Balsamo M. & Todaro M.A. 1992. Italian marine Gastrotricha: I. Six new and one redescribed species of Chaetonotida. *Bollettino di Zoologia* 59: 499–516. https://doi.org/10.1080/11250009209386711

Hummon W.D. & Todaro M.A. 2010. Analytic taxonomy and notes on marine, brackish-water and estuarine Gastrotricha. *Zootaxa* 2392: 1–32.

International Commission on Zoological Nomenclature 1999. *International Code of Zoological Nomenclature, Fourth Edition*. The International Trust for Zoological Nomenclature, The Natural History Museum, London.

Jones W.K., Hobbs H.H., Wicks C.M., Currie R.R., Hose L.D., Kerbo R.C., Goodbar J.R. & Trout J. 2003. *Recommendations and Guidelines for Managing Caves on Protected Lands*. Karst Waters Institute Special Publication, Charles Town, West Virginia.

Kånneby T., Todaro M.A. & Jondelius U. 2013. Phylogeny of Chaetonotidae and other Paucitubulatina (Gastrotricha: Chaetonotida) and colonization of aquatic ecosystems. *Zoologica Scripta* 42: 88–105. https://doi.org/10.1111/j.1463-6409.2012.00558.x

Kieneke A. & Schmidt-Rhaesa A. 2015. Gastrotricha. *In*: Schmidt-Rhaesa A. (ed.) *Handbook of Zoology. Gastrotricha and Gnathifera. Vol. 3*. De Gruyter, Berlin/Boston.

Kimura M. 1980. A simple method for estimating evolutionary rate of base substitutions through comparative studies of nucleotide sequences. *Journal of Molecular Evolution* 16: 111–120. https://doi.org/10.1007/BF01731581

Kisielewski J. 1981. *Gastrotricha from Raised and Transitional Peat Bogs in Poland*. Monografie Fauny Polski, 11. Polska Akademia Nauk, Kraków.

Kisielewski J. 1991. Inland-water Gastrotricha from Brazil. *Annales Zoologici* 43: 1–168.

Kisielewski J. 1997. *Brzuchorzeski (Gastrotricha). Fauna Słodkowodna Polski*. Zeszyt 31, Wydawnictwo Uniwersytetu Łódzkiego, Łódź.

Kolicka M. 2016. Gastrotrichs in bromeliads – newly recorded *Chaetonotus (Hystricochaetonotus) furcatus* Kisielewski, 1991 (Chaetonotida) from the Łódź Palm House. *Zoosystema* 38 (1): 141–155. https://doi.org/10.5252/z2016n1a5

Kolicka M., Dabert M., Dabert J., Kånneby T. & Kisielewski J. 2016. *Bifidochaetus*: a new Arctic genus of freshwater Chaetonotida (Gastrotricha) from Spitsbergen revealed by the integrative taxonomy approach. *Invertebrate Systematics* 30: 398–419. https://doi.org/10.1071/IS16001

Kolicka M., Jankowska E. & Kotwicki L. 2015. Baltic Sea Gastrotricha – one new species and one new record of Chaetonotida from Poland. *Zootaxa* 4027: 487–508. https://doi.org/10.11646/zootaxa.4027.4.2

Kolicka M., Kisielewski J., Kotwicki L., Zawierucha K. & Grzelak K. 2014. Checklist of Gastrotricha of the Polish Baltic Sea with the first reports of *Heterolepidoderma joermungandri* Kånneby, 2011, and *Turbanella hyalina* Schultze, 1853. *Zootaxa* 3869 (2): 101–130. https://doi.org/10.11646/zootaxa.3869.2.1

Kolicka M., Kisielewski J., Nesteruk T. & Zawierucha K. 2013. Gastrotricha from the Poznań Palm House – one new subgenus and three new species of freshwater Chaetonotida (Gastrotricha). *Zootaxa* 3717 (2): 231–279. https://doi.org/10.11646/zootaxa.3717.2.7

Leasi F. & Todaro M.A. 2008. The muscular system of *Musellifer delamarei* (Renaud-Mornant, 1968) and other chaetonotidans with implications for the phylogeny and systematization of the Paucitubulatina (Gastrotricha). *Biological Journal of the Linnean Society* 94: 379–398. https://doi.org/10.1111/j.1095-8312.2008.00974.x

Lješević A.M. 1968. *Izveštaj o speleološkim istraživanjima Lipske pećine, (elaborat) u okviru projekta "Hidrogeologija sliva Skadarskog jezera, Zavod za geološka istraživanja CG"*. Titograd.

Lješević A.M. 1969. *Izveštaj o speleološkim istraživanjima Cetinjske pećine, Zavod za geološka istraživanja CG*. Titograd.

Martel E.A. 1893. *Les abîmes: les eaux souterraines, les cavernes, les sources, la speleology: explorations souterraines effectuées de 1888 à 1893 en France, Belgique, Autriche et Grèce.* Charles Delagrave, Paris.

Martinović D. 1964. Cetinjsko polje (fizičko - geografska ispitivanja). *Glasnik Srpskog Geografskog Društva* 44: 27–37.

McCall J.N. & Fleeger J.W. 1995. Predation by juvenile fish on hyperbenthic meiofauna, a review with data on post-larval *Lelostomus xanthurus*. *Vie et Milieu* 45: 61–73.

Mihavc A. 1983. Lipska in Začirska pečina, dve veliki Črnogorski jami. Published by Jamarska Zveza Slovenje, Speleological Associaton of Slovenia. *Nase Jame* 25: 37–39.

Navajas M., Lagnel J., Gutierrez J. & Boursot P. 1998. Species-wide homogeneity of nuclear ribosomal ITS2 sequences in the spider mite *Tetranychus urticae* contrasts with extensive mitochondrial COI polymorphism. *Heredity* 80: 742–752.

Nicholas K.B. & Nicholas H.B. 1997. *GeneDoc: a Tool for Editing and Annotating Multiple Sequence Alignments.* Distributed by the author.

Nozais C., Perissinotto R. & Tita G. 2005. Seasonal dynamics of meiofauna in a South African temporarily open/closed estuary (Mdloti Estuary, Indian Ocean). *Estuarine Coastal and Shelf* 62: 325–338. https://doi.org/10.1016/j.ecss.2004.09.020

Palmer A.N. 1991. Origin and morphology of limestone caves. Vol. 103. *Bulletin of the Geological Society of America* 103 (1): 1–21.

Pešić V. 2010. *Plagigeyeria montenigrina*. The IUCN Red List of Threatened Species 2010: e.T155489A4786103. Available from http://www.iucnredlist.org/ [accessed 8 Sep. 2017].

Posada D. 2008. jModelTest: Phylogenetic model averaging. *Molecular Biology and Evolution* 25: 1253–1256. https://doi.org/10.1093/molbev/msn083

Pretner E. 1972. La biospeleologia in Jugoslavia nel dopoguerra. *Italian Journal of Zoology* 39 (4): 491–502. https://doi.org/10.1080/11250007209431403

Radulović M. & Radulović V. 2004. *Hydrogeological Map of Montenegro* 1:200,000. Geological Survey of Montenegro, Podgorica.

Rambaut A. 2014. FigTree v. 1.4.2. Available from http://tree.bio.ed.ac.uk/software/figtree/ [accessed 12 Oct. 2016].

Rambaut A. & Drummond A.J. 2007. Tracer v1.4. Distributed by the author.

Rao G.C. & Clausen C. 1970. *Planodasys marginalis* gen. et. sp. nov. and Planodasyidae fam. nov. (Gastrotricha Macrodasyoidea). *Sarsia* 42: 73–82. https://doi.org/10.1080/00364827.1970.10411164

Ronquist F., Teslenko M., van der Mark P., Ayres D.L., Darling A., Höhna S., Larget B., Liu L., Suchard M.A. & Huelsenbeck J.P. 2012. MrBayes 3.2: efficient Bayesian phylogenetic inference and model choice across a large model space. *Systematic Biology* 61: 539–542. https://doi.org/10.1093/sysbio/sys029

Roszczak R. 1969. Brzuchorzęski (Gastrotricha) środkowej Wielkopolski. Poznańskie Towarzystwo Przyjaciół Nauk. Wydział matematyczno-przyrodniczy. *Prace Komisji Biologicznej* 32 (6): 1–92.

Tamura K., Stecher G., Peterson D., Filipski A. & Kumar S. 2013. MEGA6: Molecular Evolutionary Genetics Analysis Version 6.0. *Molecular Biology and Evolution* 30 (12): 2725–2729. https://doi.org/10.1093/molbev/mst197

Telford M.J., Lockyer A.E., Cartwright-Finch C. & Littlewood D.T.J. 2003. Combined large and small subunit ribosomal RNA phylogenies support a basal position of the acoelomorph flatworms. *Proceedings of the Royal Society B, Biological Sciences* 1519 (270): 1077–1083. https://doi.org/10.1098/rspb.2003.2342

Todaro M.A. 2016. Gastrotricha [online]. Available from World Register of Marine Species at http://www.marinespecies.org/aphia.php?p=taxdetailsetid=2078 [accessed 7 May 2016].

Todaro M.A. & Hummon W.D. 2008. An overview and a dichotomous key to genera of the phylum Gastrotricha. *Meiofauna Marina* 16: 3–20.

Todaro M.A., Leasi F., Bizzarri N. & Tongiorgi P. 2006. Meiofauna densities and gastrotrich community composition in a Mediterranean sea cave. *Marine Biology* 149: 1079–1091. https://doi.org/10.1007/s00227-006-0299-z

Vandel A. 1964. *Biospeleology. The Biology of Cavernicolous Animals*. Pergamon Press, Oxford.

Manuscript received: 13 July 2016
Manuscript accepted: 19 January 2017
Published on: 28 September 2017
Topic editor: Rudy Jocqué
Desk editor: Kristiaan Hoedemakers

Appendix

Morphometric parameters of *Chaetonotus* (*Chaetonotus*) *antrumus* Kolicka sp. nov. Abbreviations: N = number of specimens or structures analysed; Range = the smallest and the largest structure measurement found among all specimens measured; SD = standard deviation. All measurements are given in micrometers (μm); all indicators are given as a percentage (%) and italicized.

Characters	N	Holotype	Range of adult paratypes	SD	N	Range of juvenile and subadult paratypes	SD
Body length	11	123.08	119.12–129.72	2.941	2	91.19–118.46	19.283
Pharynx length	11	32.79	31.85–34.85	0.966	2	30.47–31.05	0.410
Width of anterior pharynx thickening (a)	11	8.54	8.32–10.14	0.522	2	8.17–8.52	0.247
Width of pharynx narrowing (n)	11	5.81	5.06–6.22	0.367	2	5.25–5.31	0.042
Width of middle pharynx (m)	11	7.04	6.51–7.46	0.281	2	6.76–6.78	0.014
Width of posterior pharynx thickening (p)	11	9.64	9.16–11.28	0.590	2	8.84–9.05	0.148
Length of cephalic cilia (anterior tuft)	10	6.27–16.04	(5.46–6.86)–(14.54–7.21)	0.421; 0.873	2	(5.43–5.77)–(15.94–6.01)	0.247; 0.049
Length of cephalic cilia (posterior tuft)	10	8.74–18.35	(7.94–9.07)–(18.16–0.74)	0.368; 0.822	2	(8.26–8.28)–(17.82–7.96)	0.014; 0.099
Hypostomium length	10	5.29	4.56–6.08	0.438	2	4.19–5.14	0.672
Hypostomium width	10	6.58	5.73–6.97	0.395	2	5.26–6.09	0.587
Cephalion length	10	9.29	8.92–10.71	0.632	2	8.86–9.02	0.113
Cephalion width	10	8.82	8.33–9.41	0.291	2	7.81–8.40	0.417
Cephalion maximum width	10	11.37	11.14–12.18	0.375	2	10.94–11.34	0.283
Diameter of mouth ring	10	4.67	4.24–4.84	0.174	2	4.37–4.46	0.064
Furca length	10	21.71	19.77–23.24	0.868	2	20.82–21.39	0.403
Length of adhesive tube	10	10.39	10.08–11.26	0.361	2	10.02–10.07	0.035
Width of adhesive tube	10	1.29	1.26–1.34	0.029	2	1.23–1.27	0.028
Length of head scales	10	1.91–3.50	(1.57–2.19)–(3.34–3.82)	0.219; 0.182	2	(1.49–1.56)–(3.28–3.32)	0.049; 0.028
Width of head scales	10	2.04–4.14	(1.78–2.32)–(3.56–4.26)	0.207; 0.214	2	(1.62–1.69)–(3.59–3.94)	0.049; 0.247
Length of neck scales	10	1.39–3.14	(1.27–1.82)–(2.93–3.29)	0.173; 0.130	2	(1.24–1.37)–(2.89–3.06)	0.092; 0.120
Width of neck scales	10	1.66–3.05	(1.42–2.04)–(2.76–3.94)	0.195; 0.345	2	(1.47–1.57)–(2.76–2.84)	0.071; 0.057
Length of trunk scales	10	2.76–4.52	(2.47–3.02)–(4.12–5.61)	0.185; 0.453	2	(2.38–2.61)–(4.10–4.23)	0.163; 0.092

Characters	N	Holotype	Range of adult paratypes	SD	N	Range of juvenile and subadult paratypes	SD
Width of trunk scales	10	1.84–3.43	(1.64–2.04)–(3.10–4.27)	0.153; 0.347	2	(1.59–1.70)–(2.92–3.08)	0.078; 0.113
Length of small one-lobed scales	10	2.12	1.88–2.66	0.267	2	1.62–2.88	0.891
Width of small one-lobed scales	10	1.51	1.32–1.78	0.150	2	1.08–1.56	0.339
Length of furcal appendages one-lobed scales	10	4.55–4.72	(4.02–5.23)–(4.32–5.72)	0.395; 0.461	2	(3.83–4.06)–(4.09–4.27)	0.163; 0.127
Width of furcal appendages one-lobed scales	10	2.21–2.42	(2.02–2.71)–(2.08–3.17)	0.208; 0.308	2	(1.77–1.94)–(1.92–2.03)	0.120; 0.078
Length of both pairs of parafurcal scales	10	2.76–2.81	(2.04–3.38)–(2.53–3.60)	0.299; 0.324	2	(2.41–2.54)–(2.54–2.73)	0.092; 0.134
Width of parafurcal scales	10	2.27–2.34	(2.11–2.82)–(2.21–3.22)	0.239; 0.314	2	(1.87–2.04)–(2.04–2.16)	0.120; 0.085
Length of head spines	10	1.14–2.06	(1.05–1.48)–(1.83–3.09)	0.164; 0.365	2	(1.01–1.09)–(1.97–2.03)	0.057; 0.042
Length of head hair-like ventral spines	10	5.51–6.88	(5.09–6.38)–(6.38–8.55)	0.437; 0.716	2	(4.94–5.18)–(5.67–6.33)	0.170; 0.467
Length of neck spines	10	0.61–1.72	(0.47–1.26)–(1.53–2.67)	0.220; 0.329	2	(0.51–0.53)–(1.63–1.76)	0.014; 0.092
Length of neck hairlike ventral spines	10	5.36–7.24	(4.98–6.25)–(6.89–9.02)	0.430; 0.683	2	(4.57–4.97)–(6.12–6.86)	0.283; 0.523
Length of trunk spines	10	1.50–2.97	(1.33–1.94)–(2.52–4.12)	0.176; 0.448	2	(1.29–1.39)–(2.72–2.74)	0.071; 0.014
Length of trunk hair-like ventral spines	10	7.31–12.09	(7.08–9.16)–(10.49–13.96)	0.664; 1.021	2	(6.24–6.97)–(10.49–10.52)	0.516; 0.021
Length of posteriormost trunk lateral spines	10	3.77	3.39–5.93	0.721	2	3.52–3.61	0.064
Length of furcal appendages dorsal spines	10	2.64	2.42–4.08	0.530	2	2.23–2.33	0.071
Length of parafurcal spines	10	6.02	5.53–7.67	0.639	2	5.47–5.61	0.099
Length of ventral interciliary field scales	11	1.93–3.44	(1.44–1.93)–(3.08–3.72)	0.202; 0.230	2	(1.52–1.73)–(3.10–3.19)	0.148; 0.064
Width of ventral interciliary field scales	11	1.21–1.68	(1.07–1.29)–(1.56–1.88)	0.059; 0.111	2	(1.06–1.12)–(1.59–1.62)	0.042; 0.021
Length of posteriormost ventral interciliary field scales	11	5.91	5.37–6.12	0.231	2	5.46–5.62	0.113
Width of posteriormost ventral interciliary field scales	11	2.37	2.22–3.24	0.279	2	2.19–2.24	0.035
Head dorsal sensory bristles length	11	8.41	8.19–10.13	0.569	2	8.28–8.47	0.134

Characters	N	Holotype	Range of adult paratypes	SD	N	Range of juvenile and subadult paratypes	SD
Neck dorsal sensory bristles length	11	14.77	13.28–15.68	0.796	2	13.28–13.94	0.467
Posterior dorsal sensory bristles length	11	11.72	10.13–12.67	0.755	2	10.01–11.08	0.757
Length of mature egg	1	–	40.96	–	–	–	–
Width of mature egg	1		26.02		–	–	–
Number of cephalic cilia in anterior tuft	31	4	4	0	5	4	0
Number of cephalic cilia in posterior tuft	31	5	5	0	5	5	0
Number of scales in central longitudinal row	31	25	24–27	1.104	5	23–26	2.121
Total number of longitudinal alternating rows of scales	31	31	29–35	1.748	5	29–31	1.414
Number of scales in single longitudinal row on ventral interciliary field	31	3	3–4	0.467	5	3	0
Total number of longitudinal alternating rows of scales	31	9	7–9	0.809	5	9	0
Pharynx formula a	11	*26.045*	*24.317–29.096*	1.406	2	*26.312–27.962*	1.167
Pharynx formula n	11	*17.719*	*15.852–19.036*	1.028	2	*16.908–17.427*	0.367
Pharynx formula m	11	*21.47*	*20.331–22.732*	0.800	2	*21.771–22.251*	0.339
Pharynx formula p	11	*29.399*	*27.607–32.367*	1.560	2	*29.012–29.147*	0.095
Ratio of scale distribution	31	*124*	*111.5–129.6*	4.912	5	*119.2–126.1*	4.879